Master's thesis

2021

Elias Nour Boudzakhet Veidal

NTNU
Norwegian University of
Science and Technology
Faculty of Medicine and Health Sciences
Department of Clinical and Molecular Medicine

Master's thesis

Elias Nour Boudzakhet Veidal

ATM instigate melphalan mediated damage response in multiple myeloma: the tip of the iceberg

June 2021

NTNU
Norwegian University of
Science and Technology

NTNU
Norwegian University of
Science and Technology

NTNU
Norwegian University of
Science and Technology

ATM instigate melphalan mediated damage response in multiple myeloma: the tip of the iceberg

Elias Nour Boudzakhet Veidal

Master of molecular medicine
Submission date: June 2021
Supervisor: Kristian Starheim

Norwegian University of Science and Technology
Department of Clinical and Molecular Medicine

Abstract:

INTRODUCTION: Multiple myeloma (MM) is an incurable hematological cancer characterized by hyperproliferation of plasma cells. The disease's persistence is due to the development of drug resistance and relapse. The presence of minimal residual disease (MRD) after treatment is regarded as the major cause of relapse. MM cells can signal survival through pathways like NF-κB and MAPK, both under the control of the key regulator TAK1. NF-κB and MAPK activation can also lead to the production of pro-inflammatory mediators, creating a favorable environment for tumor growth. TAK1 is also considered an inhibitor of apoptosis since NF-κB is counter-regulated with RIPK1-dependent apoptosis. A pathway activated by the alkylating agent melphalan, commonly used in MM therapy. Melphalan induced irreparable DNA damage that activates TAK1, changing the destiny of the cell from apoptotic death to survival. Consequently, Inhibiting TAK1 reduces viability in myeloma cells alone and in combination with melphalan. Inhibition of TAK1 also reduces the expression of genes regulated by the oncogenic transcription factor Myc.

OBJECTIVES: This thesis examines whether melphalan activates TAK1, MAPK, and NF-κB through ATM. Test if TAK1 inhibition can neutralize the production of proinflammatory cytokines in myeloma cells. Lastly, tries to determine whether the NG25-induced reduction in Myc-controlled genes was reflected on the level of Myc-activity.

METHODS: In this study, experimental data was collected from MM cell lines by enzyme-linked immunosorbent assay (ELISA) and western blot. Western blots were used to measure protein quantity and detect protein modifications. ELISA was applied to measure the concentration of proinflammatory cytokines secreted in the medium. The cells were exposed to melphalan, NG25, or KU-55933 depending on the experimental intent.

RESULTS: Phosphorylation of ATM was observed post-melphalan in INA-6 cells. ATM inhibition reduced phosphorylation of TAK1, IκBα, and p38 in INA-6 cells. NG25 blocked the production of MCP1 in INA-6 cells. Melphalan and NG25 both reduce Myc levels in cell lines INA-6, ANBL-6, JJN3, and RPMI-8226.

CONCLUSION: Melphalan induces a DNA damage response initiated by ATM, activating NF-κB and MAPK through TAK1. TAK1 inhibition blocks the production of MCP1 and reduces Myc levels.

Acknowledgements

This master project was performed at the Institute of Clinical and Molecular Medicine (IKOM) at the Faculty of Medicine and Health Sciences and the Centre of Molecular Inflammation Research (CEMIR), Norwegian University of Science and Technology (NTNU). The work was carried out during the years 2020-2021 in the inflammatory cell death group.

First and foremost, I would like to express my very great appreciation for my main supervisor Kristian Starheim. For his patient guidance and encouragement during these not so ordinary times. For inspiring me with his enthusiasm for the research field and counseling me through the entirety of this project.

I would also like to thank the other members of our group. Ingrid Nyhus Moen for always being available, helpful in the lab, and always having some comforting words. Erling Håland for his training and guidance in the laboratory. Marie Sørensen for working alongside me, growing together to become better researchers. You have all been a great motivation to me and have a pivotal role in me completing this project.

Special thanks should also be given to the entirety of the myeloma lab, creating a welcoming environment and top-notch workplace. Everyone's willingness to give their time so generously has made this an educational experience.

Lastly, I would like to thank my friends and family. Arnfinn Øversveen for encouraging words and motivational talks. My mom and dad for supporting me and listening to my exhausted rants. And my brother for proofreading my project despite his busy schedule.

Elias N.B. Veidal
Trondheim, June 2021

Abbreviations

c-FLIP	Cellular FLICE -inhibitory protein
CCL2	C-C motif ligand 2
CCL3	C-C motif ligand 3
cIAP	Cellular inhibitor of apoptosis protein
ELKS	Proteins rich in Glutamate, Leucine, Lysine and Serine
ERK	Extracellular signal-regulated kinase
FADD	Fas-Associated protein with Death Domain
FLICE	FADD-like IL-1β-converting enzyme
IKK	IκB kinases
IL	Interleukin
IκB	NF-κB inhibitor
JNK	c-Jun N-terminal kinase
LUBAC	Linear ubiquitin chain assembly complex
MAPK	Mitogen activated kinase
MAX	Myc-associated factor X
MCP1	Monocyte chemoattractant protein 1
MEK	MAPK/ERK kinase
MIP1α	Macrophage Inflammatory Protein-1 alpha
MKK	MAPK kinase
MLKL	Mixed lineage kinase domain-like pseudokinase
MM	Multiple myeloma
MRD	Minimal residual disease
Myc	Myelocytomatosis
NEMO	NF-κB essential modulator
NES	Nuclear export sequences
NF-κB	Nuclear Factor kappa-light-chain-enhancer of activated B cells
NLS	Nuclear localization sequence
PAMPS	Pathogen associated molecular patterns
RHD	N-terminal Rel Homology domain
RIPK	Receptor-interacting protein kinases
SASP	Senescence-Associated Secretory Phenotype
TAB	TAK1-binding protein

TAD	Transcription activation domain
TAK1	TGFβ -activated kinase 1
TGFβ	Transforming growth factor Beta
TNF-α	Tumor necrosis factor alfa
TNFR1	TNF receptor type 1
TRADD	TNF receptor type 1- associated death domain
TRAF	TNF receptor–associated factor
ZSCAN4	Zinc finger and SCAN domain containing 4

IV Table of Contents

1 Introduction

1.1 Multiple myeloma

Multiple myeloma (MM) is an incurable hematological cancer, characterized by hyperproliferation of plasma cells in the bone marrow and the subsequent accumulation of monoclonal antibodies in the body (1). It accounts for 13% of hematological malignancies with an age-adjusted incidence rate of roughly 5 cases every 100 000 in the western countries. It is an affliction of the elderly, with a median age of diagnosis estimated to be 70 years (2). The disease has a comprehensive pathology, it affects the bone marrow, urinary system and blood. MM can be subdivided into active and smoldering depending on whether symptoms are present or not, respectively. The disease is considered symptomatic according to the CRAB-criteria with the presence of hypercalcemia, renal insufficiency, anemia, and bone disease. Symptomatic MM should be treated immediately, in contrast to smoldering MM where treatment has shown no benefit (1).

Myeloma cells are the result of several cytogenic irregularities in post germinal plasma cells. These cells originally inhabit the lymph nodes but will migrate back to the bone marrow. Some of the initial genetic abnormalities responsible include translocation of oncogenes like *cyclin D1* and *D3* to the immunoglobulin heavy chain locus on chromosome 14. As the disease progresses myeloma cells acquire additional mutations some of which have been studied extensively. These include deletions in the tumor suppressor *TP53* locus which code for the tumor suppressor P53. Additionally, mutations in *RAS*, hyperexpression of *BCL2,* and activation, often constitutive of Nuclear Factor kappa-light-chain-enhancer of activated B cells (NF-κB*)* (3).

The treatment of MM has drastically improved in the last decades, much due to the development of drugs like dexamethasone and bortezomib. Despite this, the disease is an incurable malignancy because of drug resistance and relapse. The presence of minimal residual disease after treatment is regarded as the major cause of relapse. This entails the survival of a minuscule number of myeloma cells in the bone marrow, which is the result of tumor heterogenicity (4). The myeloma cells make this possible by signaling through pathways important to survival, stress-response, and cell-cycle. The signaling can either be paracrine or autocrine. That is, originate from either the bone marrow microenvironment or be self-sustained with cytokines.

Myeloma cells can alternatively alter their intracellular signaling pathways to eliminate the need for such stimuli (5).

1.2 NF- κBs role in multiple myeloma

NF-κB transcription factors play a key role in the development, progression, and persistence of many cancers, including multiple myeloma (6). NF-κB regulates the transcription of genes involved in apoptosis, cell cycle control, and inflammation (7). Overactivation of NF-κB can stimulate proliferation, prevent apoptosis, render cells more tolerant to stress, and produce tumor-promoting inflammation (8). These characteristics are regarded as hallmarks of cancer (9). NF-κB is often constitutively activated in MM which provides the rationale for its importance. It contributes to MM pathogenesis through the aforementioned mechanisms (10). Additionally, many chemotherapeutics function by activating apoptosis, hence NF-κB also serves as a major cause of drug resistance (11).

The NF-κB family of proteins is comprised of the sub-units p50, p52, p65 (RelA), C-Rel, and RelB. These proteins are encoded by the genes *NF-κB1*, *NF-κB2*, *RELA*, *REL*, and *RELB* respectively. The proteins must form dimers to obtain their transcription factor activity. The NFκB-family of proteins all share an N-terminal Rel Homology domain which is responsible for this homo- and hetero-dimerization, as well as their DNA-binding capabilities (12). The transcription factor regulates a number of genes by binding the κB-site situated in promotors of these genes. These genes can be up-or downregulated by NF-κB's recruitment of coactivators or corepressors. However, only some of the subunits are capable of positive gene regulation. p50 and p52 lack a transcription activation domain and can therefore only repress gene activity, unless coupled with one of the other subunits (6).

Once dimerization occurs as a result of upstream signaling, the transcription factor translocates to the nucleus and regulates the transcription of the intended genes (6). There are two main pathways of activation for NF-κB – NF-κB1/RelA and NF-κB2/RelB (6). However, only NF-κB1 (from here termed NF-κB) is of interest to this thesis.

1.2.1 The canonical NF- κB pathway

Due to NF-κB´s importance, its activity is normally tightly regulated. The process is inducible by upstream signaling, but the signal is short-lived (7). The subunits are continually expressed and lay dormant in the cytosol, inhibited by either the Nuclear Factor of Kappa light polypeptide gene enhancer in B-cells inhibitor (IκB) family of proteins or by its own precursors (13). After pathway activation, NF-κB quickly execute its functions before regulatory mechanisms return it to a dormant state (7).

In the canonical NF-κB pathway, IκB alpha/Beta/Epsilon (IκBα, IκBβ, and IκBε) is responsible for preventing the nuclear translocation of NF-κB. This is achieved by covering the nuclear localization sequence on p65, so that its own nuclear export sequences can exclusively be accessed. The central event in canonical signaling is the phosphorylation and degradation of IκB. The canonical pathway can be initiated by a wide range of inflammatory molecules such as cytokines, pathogen-associated molecular patterns (PAMPS), and antigens (13). The different receptors utilize different adaptor proteins for furthering the signal, but a pillar of canonical NF-κB signaling is the formation of large protein complexes, often polyubiquitinated (14).

Canonical signaling is also called NEMO-dependent because NEMO (NF-kappa-B essential modulator) is one of the central contributors to furthering a signal that eventually leads to phosphorylation of IκB-proteins and subsequent degradation. NEMO works as a scaffold for the involvement of IκB kinases, IKKα and IKKβ. They are recruited by polyubiquitylation (K63) of NEMO and can be activated in several ways (Figure 1.1). One being multimerization of the IKK-proteins by NEMO, leading to trans-autophosphorylation. Alternatively, NEMO can also guide them within proximity of upstream kinases. Lastly is the formation of large protein complexes often initiated by linear polyubiquitination of NEMO. Modifications supplied by the linear ubiquitin chain assembly complex (LUBAC) (13).

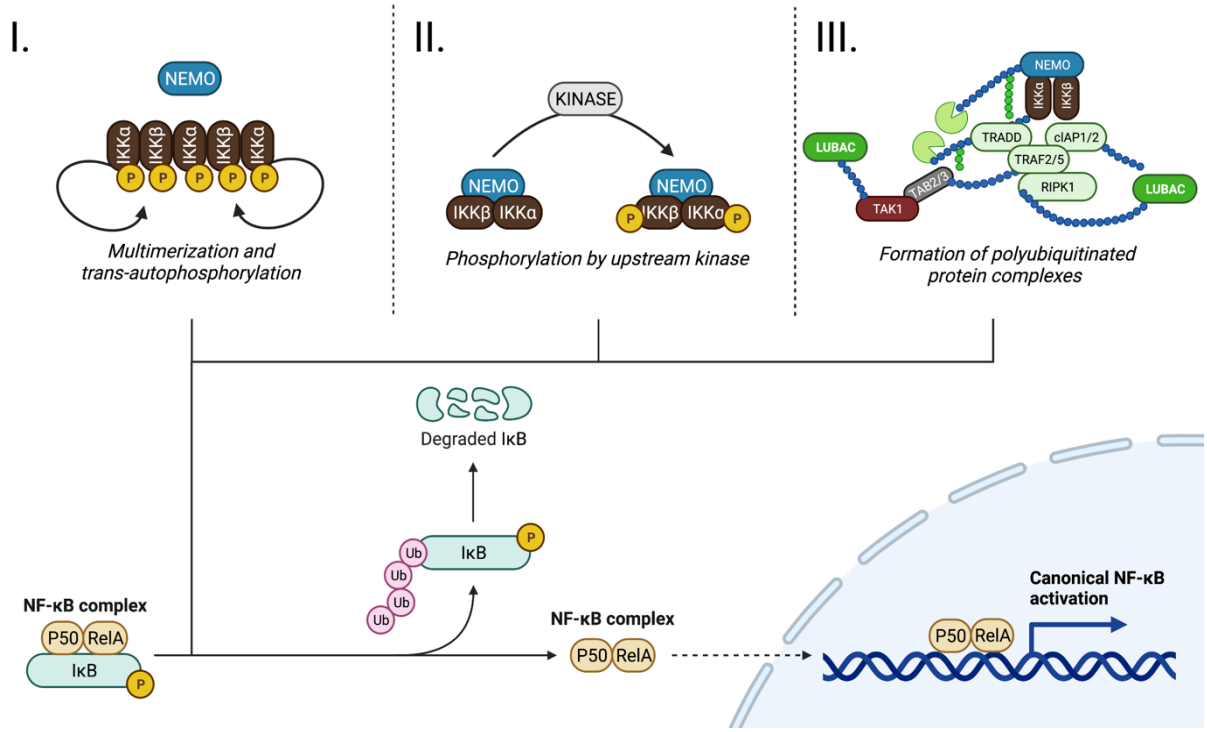

Figure 1.1 NEMO activation of IKK IκB kinases. Upon poly-ubiquitylation of NEMO, IKKα and IKKβ are recruited. Their activation can occur in three distinct ways. **I.** Multimerization triggering trans-autophosphorylation. **II.** Phosphorylation by an upstream kinase. **III.** Formation of large protein complexes. All leading to the phosphorylation and ubiquitination of IκB inhibitors, marking them for proteasomal degradation. An event that allows for NF-κB nuclear translocation and gene regulation (13).

When NEMO has engaged IKKα and IKKβ, this phosphorylation can occur. Which produces a signal leading to subsequent ubiquitination (K47) marking the inhibitors for proteasomal degradation (13). When released, NF-κB dimer formation is made possible, when canonical signaling is concerned this is mainly the RelA/p50-dimer (14).

1.2.2 RIPK's role in NF- κB signaling

A subset of canonical NF-κB-signaling is dependent on a family of proteins called Receptor-interacting protein kinases (RIPK's). This family consists of 7 proteins, characterized by their serine/threonine kinase domains. However, only RIPK 1, 2, and 3 seem to be related to NF-κB signaling, the latter of lesser importance with a role in inhibiting RIPK1. They excerpt their protein binding abilities upstream and in concert with tumor necrosis factor receptor-associated factor (TRAF) proteins. The span of RIPK's involvement includes most TRAF-dependent signaling but may also include TRAF-independent pathways like in DNA damage. RIPK proteins are kinases, but this activity is not required for IKK-activation. Instead, they have a scaffolding role. They are responsible for initiating complex formation, which in turn leads to autophosphorylation of IKK proteins (12).

This complex formation requires modification of RIPK1, more specifically K63- and M1-linked polyubiquitination (15). K63-ubiquitination is catalyzed by the E3-ubiquitin ligases cellular inhibitor of apoptosis protein 1/2 (cIAP 1/2). Their activity is also responsible for the recruitment of LUBAC which conducts M1- modification. The ubiquitin-chains on RIPK1 engage downstream proteins and serves as a docking site for complex formation. Complexes such as the IKK-complex, consisting of NEMO, IKKα, and IKKβ. As well as the transforming growth factor β (TGFβ) -activated kinase 1 (TAK1) - complex which will be described in more detail later. This particular modification is the crossroad of life and death for the cell. Ubiquitin ligation on RIPK1 signals survival through NF-κB. De-ubiquitination however, initiates RIPK-dependent cell death (16).

1.2.3 RIPK1 can direct the cell to undergo apoptosis and necroptosis

RIP-mediated apoptosis, also referred to as the extrinsic pathway is illustrated by the well-studied cytokine tumor necrosis factor alfa (TNF-α) (Figure 1.2). Following the binding of its respective receptor tumor necrosis factor receptor 1 (TNFR1), several adaptor proteins form a complex with the intracellular segment of the receptor. These proteins include tumor necrosis factor receptor type 1-associated death domain (TRADD), TRAF 2/5, cIAP 1/2, and RIPK1, entitled Complex I. TRAF and cIAP proteins are ubiquitin ligases and modify RIPK1 thereby activating the NF-*κ*B-pathway (17).

The alternative to this is signaling apoptosis, which is triggered by the deubiquitylation of RIPK1. Induction of deubiquitinases CYLD and A20 leads to the formation of a second complex (18). One that includes Fas-Associated protein with Death Domain (FADD), RIPK1, and caspase-8. This complex formation causes homodimerization and autocleavage of caspase-8. An active caspase-8 initiates an activation cascade of downstream caspases like caspase-3 (17). Further cleavage occurs of protein kinases, structural proteins, and DNA-repair mechanisms, in addition to cleavage of inhibitors of DNases which causes nuclear fragmentation. Terminally leading to the distinct morphological changes of apoptosis, like the formation of apoptosomes (19).

NF-*κ*B and RIP-mediated apoptosis are co-regulated pathways. Activation of NF-*κ*B leads to the transcription of inhibitors of apoptosis. Inhibitors including cellular FADD-like IL-1β-converting enzyme (FLICE) -inhibitory protein (c-FLIP) and cIAP (16). c-FLIP mimics caspase-8, it is structurally similar but lacks the catalytic activity. Caspase-8 form dimers and

activate by autoproteolytic cleavage, though this reaction is halted by the binding of c-FLIP. cIAP-family proteins also inhibit apoptosis, directly interacting with downstream caspases like caspase-3 (17, 18). NF-κB also upregulates the expression of proteins that terminate NF-κB activation in a negative feedback fashion. Proteins like IκB which will bind and inhibit NF-κB; and A20 which remove RIPK1 ubiquitination (18).

The third option in addition to NF-κB and apoptosis is another form of programmed cell death called necroptosis. Caspase-8 cleaves RIPK1 and blocks its kinase activation during apoptotic activation. If Caspase-8 is inhibited pharmaceutically, or by the earlier mentioned cFLIP, but RIPK1 is deubiquitinated, it will form complex with and phosphorylate RIPK3 (Complex III). RIPK3 will then go on to phosphorylate mixed lineage kinase domain-like pseudokinase (MLKL), leading to subsequent oligomerization. Creating a structure that can permeabilize the plasma membrane and organelles, leading to rupture (17).

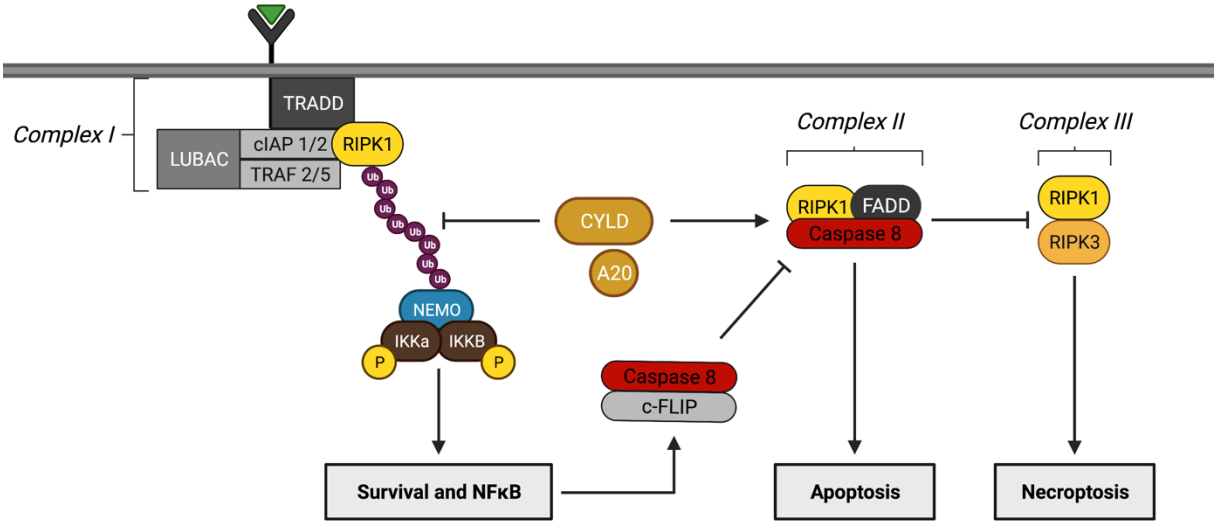

Figure 1.2 RIPK1 modification regulate NF- κB, apoptosis, and necroptosis. Upon TNF-α stimulation of TNR1, an intracellular membrane-bound complex forms. Complex 1 contains TRADD, TRAF 2/5, cIAP 1/2, and RIPK1. If RIPK1 is ubiquitinated by LUBAC, TRAF, and cIAP the cell signals NF- κB through the IKK-complex and TAK1 (not shown). If RIPK1 is deubiquitinated by CYLD and A20 the cell signals apoptosis. However, this depends on caspase 8 availability regulated by c-FLIP an off product of NF- κB. If Caspase 8 is available Complex 2 is formed by RIPK1, Caspase 8, and FADD. If not, a third complex form with RIPK1/3 that signals necroptosis (16).

1.2.4 TAK1, a key regulator of NF- κB and MAPK

TAK1 or MAP3K7 regulates RIPK1 through NF-κB and its inhibition is sufficient to activate programmed cell death in myeloma cells (20). It also regulates several pathways important to cellular processes. These include redox homeostasis, microtubule modification, development, and morphogenesis. More importantly, signaling survival through NF-κB and directing the cellular stress-response through mitogen-activated kinase (MAPK) (21) (Figure 1.3). TAK1 is

activated by several stimuli including exogenous ligands like PAMPS, IL-1, and TNF- α, but also endogenous stimuli like genotoxic stress. TAK1 is a kinase and therefore phosphorylates its substrates. Its catalytic activity however is not present without the formation of a complex with the co-enzymes TAK1-binding proteins 1-3 (TAB1-3). The formation of the TAK1-complex, consisting of TAK1-TAB1 and either TAB2 or TAB3, leads to autophosphorylation and activation (22). When activated, TAK1 phosphorylates IκBα and marks it for degradation in the proteasome. NF-κB is then released and translocated to the nucleus where it can modulate the transcription of genes. Additionally, TAK1 also indirectly activates the MAPK's p38, c-Jun N-terminal kinase (JNK), and extracellular signal-regulated kinase (ERK) (23).

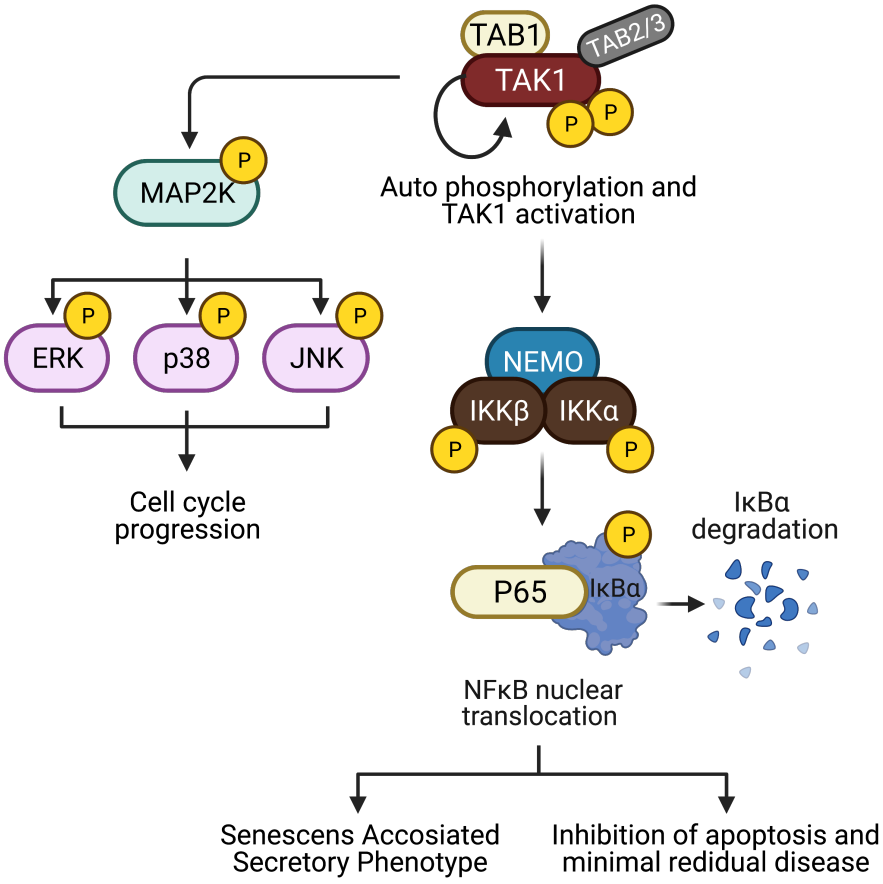

Figure 1.3 The TAK1-complex activate NF-κB and MAPK signaling. Upon upstream signaling TAK1 is activated by complex formation with TAB1 and either TAB2 or TAB3. This complex initiates autophosphorylation of TAK1 activating its catalytic activity. TAK1 goes on to phosphorylate downstream intermediates as the IKK-complex and MAP2Ks. They again phosphorylate IκBs and MAPKs ERK, p38, and JNK respectively. This activation concludes with gene regulation by a multitude of transcription factors and belonging consequences (22).

1.2.5 MAPK's the second strategy of survival

MAPK's are conserved serine-threonine kinases involved in a variety of cellular processes (24). The pathways are complex, but they all share a similar structure in transmitting a signal. Each family having a hieratical structure containing three MAPK's acting unintermittedly. First, MAPKK kinases (MAPKKK) are phosphorylated as a result of upstream stimuli. This activation allows it to phosphorylate MAPK kinases (MAPKK), which activate the concluding MAPK's by dual phosphorylation of tyrosine and threonine residues. MAPK's can then go on to phosphorylate target substrates like phospholipases, transcription factors, and cytoskeletal proteins with a wide range of functions (25).

To date, five groups have been established, but the most studied are ERK1/2, JNK, and p38. The ERK kinases are usually activated in response to growth factors, mitogens and coherently regulate functions related to cell growth and proliferation. While JNK and p38 are engaged in response to different types of stress and cytokines. They control the nuclear response to cellular stress among other things (24). ERK family kinases are activated by MEK1 and MEK2; JNK by MKK4 and MKK7; and p38 by MKK3 and MKK6. All MAPKK's that are substrates of TAK1 (17, 22, 26). The MAPK- cascade is a critical pathway for survival, resistance, and proliferation of cancer cells (27). It also affects other parts of the myeloma pathology, for instance, p38 is responsible for osteolysis (28).

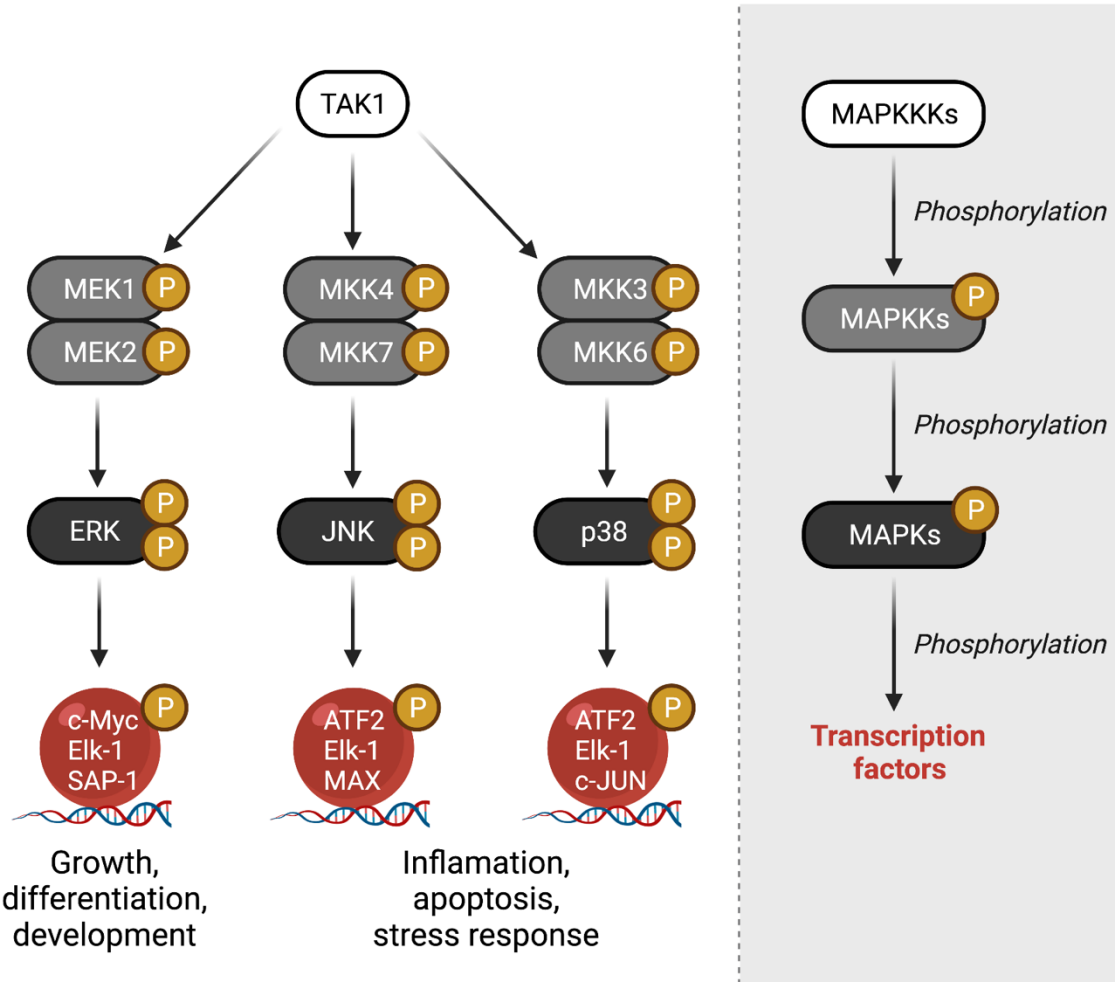

Figure 1.4 MAPK cascades transduction of signals to cellular responses. Upon stimulation, these signaling pathways signal through a similar hieratical structure. Starting with MAPKK kinases such as TAK1 which phosphorylate MAPK kinases like MEKs and MKKs. These go on to dually phosphorylate MAP kinases like ERK, JNK, and p38. These can phosphorylate target substrates regulating cellular processes.

1.3 Myc in multiple myeloma

Myc also called c-myc, is an oncogenic transcription factor of the *MYC* family (29). When activated it forms heterodimeric complexes with Myc-associated factor X (MAX) (30). This Myc-Max complex binds to regulatory sequences called E-boxes on genes and recruit transcriptional co-activators (29). Together they regulate biological functions including cell cycle, proliferation, growth, transcription, translation, metabolism, and cell death (30). It has been implicated in almost all parts of the cell cycle by targeting transcription of cell-cycle regulators (29).

An increase in Myc stimulates, whereas a decrease inhibits cell-cycle progression (29). *MYC*-genes are dysregulated in a broad range of cancer and is estimated to be elevated in up to 70% of all human cancers (30, 31). In MM, Myc is partly responsible for transitioning from earlier stages of the disease. Myc activation is present in 67% of MM whether it be due to

translocations, increased gene copy number, or mutations in important pathways like MAPK. *MYC* has also been shown to be co-regulated with NF-κB in B- and plasma-cell cancers (32).

1.4 Melphalan as treatment of multiple myeloma

Melphalan is a chemotherapeutic used in treatment of MM, classified as an alkylator. Alkylators are DNA-damaging agents that are widely used in the treatment of MM. Alkylating agents exert their cytotoxic effect by binding the DNA and adding an alkyl group to the guanine bases. Particular for melphalan is its ability to form both inter-and intra-strand crosslinks, therefore it's termed a bifunctional alkylating agent. The crosslinks eventually lead to base deletions, strand breaks, and ring formations that can halt replication (33).

Melphalan was first utilized to treat MM in 1958 and has since been employed as the standard treatment for elderly patients, as well as in combination with autologous transplant for younger patients (33). Even though many novel therapeutics have since been developed, alkylators remain relevant because of drug resistance (34). Melphalan targets highly proliferative cells and causes irreparable DNA damage which in turn can cause apoptosis, predominantly through the intrinsic mitochondrial apoptosis pathway. In parallel, this kind of genotoxic stress also triggers NF-κB signaling, and the balance between death-and survival signals decide the cells faith (35).

1.5 Genotoxic stress-induced by DNA-damaging agents

NF-κB activation can be a response to several different stimuli, including cytokines, growth factors, and pathogens. Myeloma cells are therefore greatly influenced by the cytokines present in the bone marrow. It can also be activated by intracellular signals like genotoxic stress. Several studies show that genotoxic drugs activate NF-κB through an ATM-TAK1 signaling cascade (36-38). Most relevant for this thesis is the DNA damage induced by melphalan. Typically, such a signal is initiated by the nuclear DNA-sensor Serine/threonine kinase (ATM). ATM activation, complex formation with NEMO, and cytosolic translocation leading to activation of TAK1 (22, 36). However, this has not yet been shown for the drug melphalan or in myeloma cells.

DNA-damaging agents can cause downstream activation of TAK1 in two distinct ways, both beginning with ATM-NEMO complex formation. In the first pathway, they recruit the ubiquitin conjugation system, consisting of like X-linked Inhibitor of Apoptosis (XIAP) and Ubiquitin-Conjugating enzyme 13 (Ubc13). This initiates ubiquitination of ELKS (Proteins rich in Glutamate, Leucine, Lysine, and Serine) eventually leading to TAK1 activation. In this pathway, NEMO has a dual role. It is first present in the ATM-NEMO complex upstream of TAK1, then binding ELKS-bound Ubiquitin to orchestrate TAK1 activation of the IKK-complex (37). The second pathway leads to K63-ubiquitination of RIPK1 rather than ELKS. RIPK1 then recruits the TAK1 complex leading to subsequent autophosphorylation and activation. However, RIPK1 required SUMO-1 modification to engage TAK-1 (36).

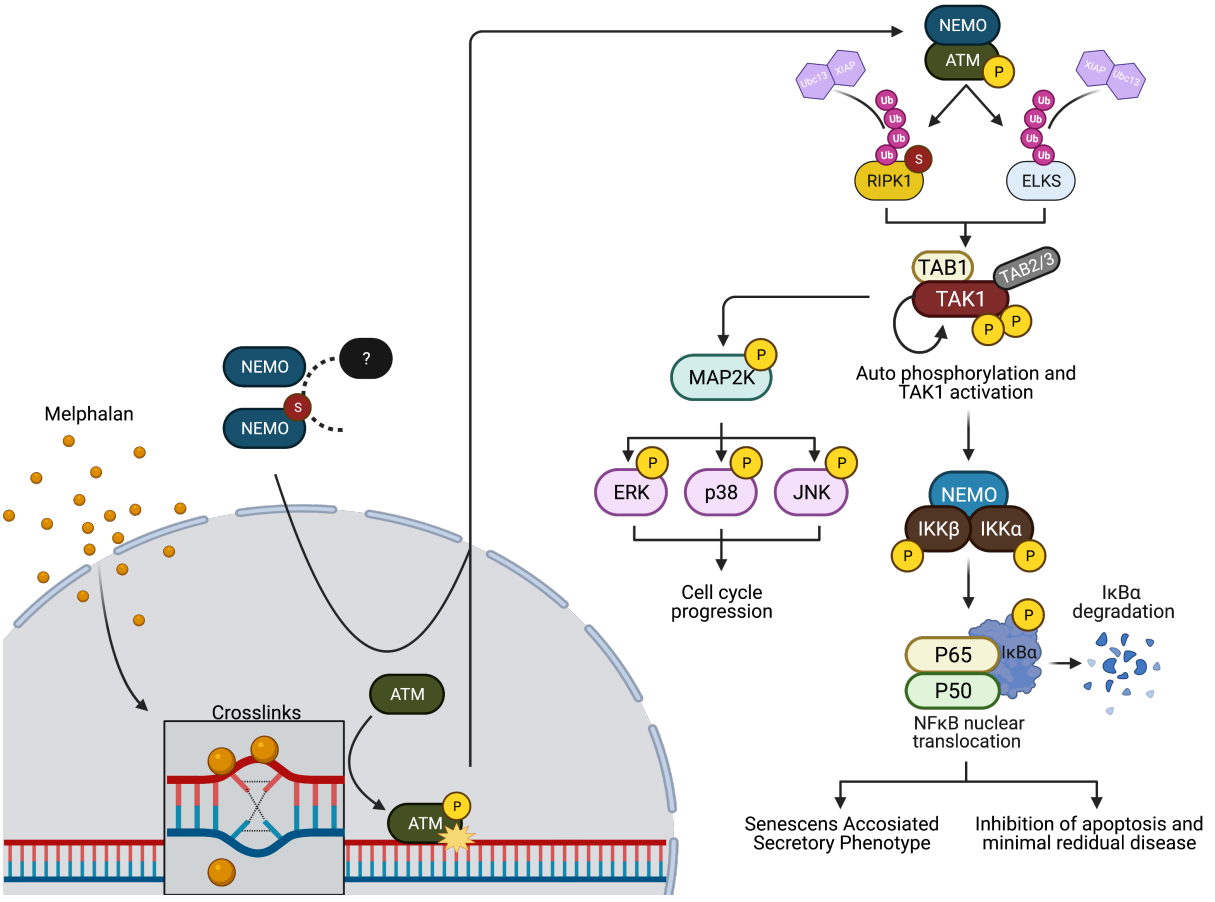

Figure 1.5 Hypothetical illustration of the DNA damage response caused by melphalan. Melphalan induces inter- and intra-strand crosslinks by adding alkyl groups to the guanine bases of DNA. This initiates autophosphorylation of ATM and complex formation with NEMO. Beforehand NEMO is SUMOylated for nuclear passage. The complex recruit's ubiquitination ligases XIAP and Ubc13 which modify either ELKS or RIPK1. The TAK1-complex is formed, and auto phosphorylation occurs. TAK1 signals through MAPKs and NF-κB.

1.6 Therapy Induced Senescence

Another emerging role of NF-κB, especially considering genotoxic insults is the development of senescent cells with a proinflammatory phenotype (39). Senescence-Associated Secretory Phenotype (SASP) describes the ability of some senescent cells to secrete cellular regulators like cytokines, chemokines, proteases, growth factors, and bioactive lipids. NFκB directs several genes that lead to cytokine secretion like ZSCAN4 (Zinc finger and SCAN domain containing 4) (40). ZSSCAN4 is elevated after transduction by ATM and TAK1 during acute DNA damage responses. Likewise, TAK1 activation can elevate ZSSCAN4 through p38 to support persistent SASP-development (41).

The role of senescent cells is to prohibit proliferation and cell growth in undesirable cells. SASP, in contrast to other senescent cells, uphold their metabolic activity and are somewhat resistant to cell death. They express a fixed cell cycle-arrest, but accumulating evidence suggests that they can have the capacity to escape this state (42, 43). With age, these cells accumulate, and in older primates they constitute between 5-20% of their cells. This is significant because they strongly outnumber the professional secretory cells and therefore, set the stage for the physiological environment in our body (43).

This is especially interesting concerning tumor growth since the properties of SASP induced cells can be both tumor-suppressing and mediating, not to mention that they themselves can be tumorous (40). Some forms of chemotherapy can also result in therapy-induced senescence (TIS). Allowing the malignant cells to live on with this phenotype. SASP is characterized by secretion of cellular regulators, cell-cycle arrest, and resistance to cell death. The secretome varies somewhat between SASP-cells, but it usually contains proinflammatory cytokines such as IL (Interleukin)- 6/8/1, MIP1α, and MCP1 (43). This reinforces the phenotype and promotes a low-grade inflammation that promotes survival and reduces drug sensitivity (44). Through mutations in the NF-κB signaling pathways or cytokine stimulation from the surrounding micro-environment – can MM-cells utilize NF-κB's properties to counteract the effects of commonly used drugs like melphalan (6). TIS has now been established as a response to many chemotherapeutics and hence, is a target for cancer therapy (42).

1.7 Targeting TAK1 in Multiple myeloma

The transcription factor NF-κB is overexpressed and even constitutively active in MM cells, both in cell lines and patient samples. Lower levels of NF-κB activity are related to treatment sensitivity, while higher levels to resistance and relapse (45). Therefore, TAK1 can be considered a viable candidate as a drug target. As demonstrated in many forms of cancer, TAK1 inhibition leads to death of tumor cells due to its key role in inhibiting apoptosis. In combination with pro-apoptotic mediators TAK1-inhibitors can lead to cancer remission and abrogate resistance to therapy (22).

TAK1`s potential as a drug target is also substantiated by other drugs directed at myeloma-cells dependence of NF-κB signaling. Such as bortezomib the proteasome inhibitor (33), IAP-antagonists (46), and other drugs that have shown potential in the clinic in combination with conventional chemotherapeutic agents like melphalan. In addition to removing the minimal residual disease, can combinational therapy with new drugs, also lower the dose required for treatment with the unquestionably toxic melphalan. This would be valuable for an at-risk elderly patient base (33, 47).

1.8 Aim of the study

Data required by our research group demonstrates that TAK1 inhibitors 5z7 and NG25 reduce cell viability and induce apoptosis both in combination with melphalan and independently in MM cell lines and patient samples. Melphalan activates the pro-survival pathways NF-κB and MAP kinases p38 and JNK, and these are blocked by TAK1-inhibitors. How melphalan activates TAK1 in MM has not been yet determined (Håland, *Unpublished*).

MAPK and NF-κB regulates both SASP and cell cycle control. RNA-sequencing data also showed that NG25 reduced transcription of Myc-controlled genes, including genes involved in cell cycle control, this was consistent with the role of TAK1 in MAPK control, but more experiments were needed to further validate these results (Håland, *Unpublished*).

Therefore, the main aim of this thesis was as following:

- Determine whether melphalan activates TAK1, MAPK, and NF-κB through ATM.
- Test if TAK1 inhibition can neutralize the production of SASP cytokines in myeloma cells.
- Test whether the NG25-induced reduction in Myc-controlled genes was reflected on the level of Myc-activity.

2 Material and Methods

2.1 Cell culture conditions and stimulation

All the experiments performed for this thesis were done on human multiple myeloma cell lines. The abovementioned cell lines were supplied by the Center for myeloma research, NTNU. The cell lines used for this thesis include: INA-6, ANBL-6, JJN-3, and RPMI-8226. The cells were cultured in their respective medium illustrated in Table 1 and were kept in cell-culture bottles in 37°C humidified incubators with 5% CO_2.

Table 1: Cell lines and the medium used for culturing

Cell line	Medium
INA-6	Dulbecco's modified Eagle medium supplemented with 10% Fetal Calf Serum (FCS), L-Glutamine, and 1 ng/ml interleukin (IL)-6
ANBL-6	Dulbecco's modified Eagle medium supplemented with 10% FCS, L-Glutamine, and 1 ng/ml IL-6
JJN-3	Dulbecco's modified Eagle medium supplemented with 10% FCS and L-Glutamine.
RPMI-8226	Dulbecco's modified Eagle medium supplemented with 20% FCS and L-Glutamine.

In preparation for experiments, the cells were transferred to new 50ml tubes and centrifuged at 1500 x g for 8 minutes to spin down the cells creating a pellet. The supernatant was then removed, replaced by 20ml new medium following resuspension. The cells were thereafter counted using a Z2 Counter (Beckman Coulter Inc.). When calculations were made the appropriate number of cells could be seeded out on plates and stimulated according to the experimental conditions required. Table 2 includes the compounds used as treatment in this thesis.

Table 2: Treatment and stimuli used for experiment preparation

Compound	Mechanism of action	Manufacturer	Catalog number
Melphalan	Alkylator, induce DNA damage	Sigma-Aldrich	MG-2011
NG25	ATP-competitive inhibitor of TAK1	MedChem Express	HY-15434
5z-7-Oxozeaneol	ATP-competitive irreversible inhibitor of TAK1	Sigma-Aldrich	253863-19-3
Ku-55933	ATM-kinase inhibitor	MedChem Express	16872
Ethanol	Negative control, diluent for Melphalan	Thermo Fisher Scientific	T08204K7
DMSO	Negative control, diluent for NG25, Ku-55933 and 5z-7-Oxozeaneol	Sigma Life Science	D2650

2.2 Cell lysis, SDS-Page, and Western blotting

Sodium dodecyl sulfate-polyacrylamide gel electrophoresis (SDS-PAGE gel) and western blotting were used to detect and characterize specific proteins and their respective PTMs in protein extracts derived from myeloma cell lines. The protocol was executed on ice and with a centrifuge temperature of 4°C to prevent proteolysis. After cell preparation, treatment and incubation the cell lysis was performed as follows. First, the cells were transferred to Eppendorf tubes and marked with treatment specifications. The tubes were then centrifuged at 800xg for 5 minutes, the supernatant containing medium was then removed and washed by resuspension of 1000µl Phosphate Buffered Saline (PBS). The cells were soon after centrifuged and PBS discarded. Cells were lysed by resuspending the pellet in Lysis buffer.

A lysis buffer prepared in advance, containing 1% Nonyl Phenoxypolyethoxylethanol (NP-40), 150 mM NaCl, 50 mM Tris-HCl (pH 8), 10% Glycerol and 1mM Ethylenediaminetetraacetic acid (EDTA). Before use, the buffer was added protease inhibitor (cOmplete Mini EDTA- free, Roche Life Science, #11873580001) and phosphatase inhibitors Sodium fluoride (NaF, 25 mM) and Sodium orthovanadate (Na_3VO_4, 1 mM), in order to prevent protein degradation by proteases and phosphatases. In some instances, N-Ethylmaleimide (NEM), a deubiquitinase inhibitor, was also added to preserve the ubiquitination patterns.

The tubes with added lysis buffer were incubated on ice for 15 minutes followed by an equal time of centrifugation on 15 000 g to remove DNA and membranes. New Eppendorf tubes were prepared with LDS Sample buffer containing sodium dodecyl sulfate (SDS, NuPage Invitrogen, #NP0007) added Dithiothreitol (DTT, 1:10) with a combined volume of 1:4 that of the lysate. The supernatant was transferred to the new tubes and incubated for 10 minutes on 80 ^{O}C heating blocks (QBD2, Grant A/S) to denature the proteins. SDS works as a detergent, binding the peptides making them negatively charged. DTT is used to disrupt the disulfide bonds breaking up the tertiary and secondary structure of the peptide. The protein's uniform structure makes it possible to measure the peptide length proportional to the protein's migration in gel. The lysate could then be stored at -80 ^{O}C.

The proteins were separated in Bis-Tris (4-12% polyacrylamide) separating precast-gels (Life Technologies, #NP0321BOX) in Xcell Surelock Mini-Cell (NuPage, Life Technologies, #EI0001) electrophoresis systems with 1x MOPS running-buffer (NuPage, #NP0001). The gel was loaded with cell lysates and See Blue Protein standard (ThermoFisher Scientific, #LC5925) to be used as a reference ladder. The gel was run on different programs according to the molecular weight of the protein of interest. The separated proteins were then transferred to a nitrocellulose membrane, by sandwiching the gel in iBlot™ 2 Transfer Stacks (ThermoFisher Scientific, #IB23001) and dry-blotting in an iBlot™ 2 Gel Transfer Device (ThermoFisher Scientific). The specifications of the western blotting and gel-electrophoresis are illustrated in Table 3 below. Different program specifications for different proteins were deduced through optimization of the protocol. Different gel electrophoresis program settings to obtain optimal separation of protein. Different western blotting program settings to ensure that larger proteins were transferred to the membrane as they require more time to transfer from gel to membrane.

Table 3: Program specifications for western blotting and gel electrophoresis

	Gel electrophoresis	Western blotting
Large proteins (90kDa<)	Step 1 (80V, 30min) Step 2 (150V, 30min) Step 3 (180V, 3 hours)	Step 1 (20V, 21min)
Medium proteins (30-90kDa)	Step 1 (100V, 30min) Step 2 (150V, 90min)	Step 1 (20V, 4min) Step 2 (23V, 4min) Step 3 (25V, 2 min)
Small proteins (30kDa>)	Step 1 (100V, 30min) Step 2 (150V, 90min)	Step 1(20V, 1min) Step 2(23V, 4min) Step 3(25V, 2 min)

The membrane was blocked with 5% Bovine serum albumin (BSA) in tris-buffered saline (TBS) with 0.1% Tween-20 (TBST) for 1 hour at room temperature to prevent unspecific binding of the antibodies. Thereafter, the membrane was incubated overnight with primary antibodies for the proteins of interest. Some antibodies required more incubation time, especially those for larger and/or phosphorylated proteins that were harder to transfer or detect. The loading control used for this thesis was the housekeeping protein β-tubulin and required only 1-hour incubation because it is present in larger quantities. Loading control is necessary to normalize the values with the total protein content in the sample. All the primary antibodies used in this thesis are listed in Table 4 below.

Table 4: Primary antibodies used for Western blot staining:

Protein target	Species	Molecular weight	Manufacturer	Catalog number
Phospho-ATM(Ser1981)	Rabbit	350kDa	Cell Signaling Technology	5883S
NEMO/IKKγ	Mouse	48kDa	Santa Cruz Biotec	166398
RIPK1	Rabbit	76kDa	Cell Signaling Technology	3493S
Phospho- IκBα(Ser32)	Rabbit	36kDa	Cell Signaling Technology	2859S
Phospho-TAK1(Thr184/187)	Rabbit	82kDa	Cell Signaling Technology	4508S
Phospho-p38 (Thr180/Thr182)	Mouse	38kDa	Cell Signaling Technology	9211S
Myc	Rabbit	70kDa	Cell Signaling Technology	D84C12
β-tubulin	Rabbit	55kDa	Abcam	ab6046

Primary antibodies were followed by three, 5-minute washing steps with TBST before secondary antibodies were applied to the membrane. The membrane was incubated with secondary antibodies at room temperature for one hour. Then it was rinsed by repeating the three washing steps, followed by 4 minutes with Super Signal horseradish peroxidase based chemiluminescence (Thermo Fisher, 1:1, #34096) western blot enhancer before the blots were visualized on an Odyssey LI-COR Fc system.

Loading Control with β-tubulin was done with fluorescent secondary antibodies. This to prevent cross-reactivity with proteins near 55kDa, in addition to having a larger linear range which is more appropriate with strong signals. Also, this requires only an hour of incubation with primary antibodies. The membranes with fluorescent antibodies were developed in an Odyssey LI-COR CLx system. The secondary antibodies used are listed in Table 5.

Table 5: Secondary antibodies used for western blot staining:

Antibody Target	Species	Conjugate	Manufacturer	Catalog number
Polyclonal Goat Anti-Mouse immunoglobulin IgG HRP	Goat	HRP	Dako Denmark A/S	P0447
Polyclonal Goat Anti-Rabbit Immunoglobulin IgG HRP	Goat	HRP	Dako Denmark A/S	P0448
IRDye® 680RD Goat-anti-Mouse Antibody	Goat	Fluorescence	LI-COR A/S	D00819-05

2.3 Enzyme-linked immunosorbent assay

Enzyme-linked immunosorbent assay (ELISA) is a method for detecting and quantifying soluble substances such as peptides, proteins, antibodies, and hormones. Of interest to this thesis was the proinflammatory cytokines secreted by myeloma cells. The cells were prepared in 96-well plates and treated in technical triplicates as described above. Cells were then centrifuged at 1500 x g for 5 minutes. The medium was collected and transferred to a new plate; the cells were discarded. Supernatant could be analyzed by ELISA immediately, or stored at -20°C. Reagents used for these experiments were Purchased by R&D Systems. ELISA-kits for each protein of interest and are listed below in Table 6.

Table 6: R&D Systems ELISA-kits used for supernatant analysis

Protein target	Species	Manufacturer	Catalog number
MCP-1	Human	R&D Systems A/S	#DY279
MIP1α	Human	R&D Systems A/S	#DY270

The modified protocol used here halved the volume of each reagent in the belonging COA-sheet. ELISA 96 F-well immuno-plates (Thermo Fisher, #7905) were coated with capture-antibodies diluted in PBS and incubated at room temperature overnight. The plate was washed on a Tecan 96PW microplate-washer and blocked for 1-hour at room temperature to prevent unspecific binding. The blocking agent used was called reagent diluent and contained 10% BSA in PBS. After blocking the washing were repeated before the plates was incubated with supernatant or protein standard for 2-hours at room temperature.

Both supernatant and protein standard were done in technical triplicates. The protein standard served as a reference since the concentration applied is already known. The plates were washed once again followed by 2-hours incubation with detection antibodies. These antibodies have conjugated biotin molecules. Again, the plates were washed and incubated with Streptavidin-HRP and then Substrate Solution (1:1 H_2O_2 and Tetramethylbenzidine), each for 20 minutes at room temperature. Streptavidin binds the biotin molecules, this allows the HRP-enzyme to gain its catalytic activity. So, when its chromogenic substrate is added, the oxidization of the substrate produces a measurable color change. Tetramethylbenzidine is turned into a blue oxidation product. To terminate the enzymatic reaction, Stop Solution namely sulphuric acid (VWR Chemicals, #UN2796) were added. Sulphuric acid lowers the pH in medium, to one outside the working range of HRP. Additionally, the blue oxidation product is turned into a yellow derivate, with a significantly higher molar absorptivity. The plate was so visualized on an iMark™ Microplate Absorbance Reader.

2.5 Statistics

All ELISA experiments executed for this thesis were performed with both technical triplicates and three identical, but independent repetitions. For these experiments, figures are produced from the entirety of the data, encompassing all repetitions. Western blots are performed in three identical, but independent experiments. Figures consist of one representative membrane and figures constructed from the entirety of quantifications, encompassing all repetitions. In this case, the remaining repetitions are summarized in the supplementary section. The data were analyzed with Student t-tests for pairwise comparison and ANOVA-test for more conditions with Tukey-test for pairwise comparison of multiple groups. Both tests with a cut-off value of $0{,}05 \geqq p$ for statistical significance. In the figures, asterisk marks statistical significance compared to the negative control, while double asterisk marks between groups. Standard deviations from the different replications are illustrated by whiskers. However, some experiments lack the proper number of replications due to time constraints. These lack statistical analysis and this will be indicated in Figure-text.

3 Results

3.1 Melphalan-induced stress and the proteins involved in INA-6 cells

Data from our group show that melphalan induces the activation of TAK1 and downstream proteins (Håland, *Unpublished*). The proposed mechanisms for the DNA-damage response involve several main culpants and their respective modifications. Among these, ATM, RIPK1, and NEMO are frequently cited (36). To test whether these are responsible for the signal transduction caused by sublethal doses of melphalan in myeloma cells, the following was done. INA-6 cells were seeded and treated in a time series with 10uM melphalan for either 2-, 4- or 6-hours. Then the cells were lysed to assess protein-quantity and potential PTM's with western blot analysis. A more detailed account of the protocol specification is described in the method section. Three independent experiments are performed for each protein. One representative experiment is shown and a complete set of membranes for all experiments are given in Supplementary Figure 1.

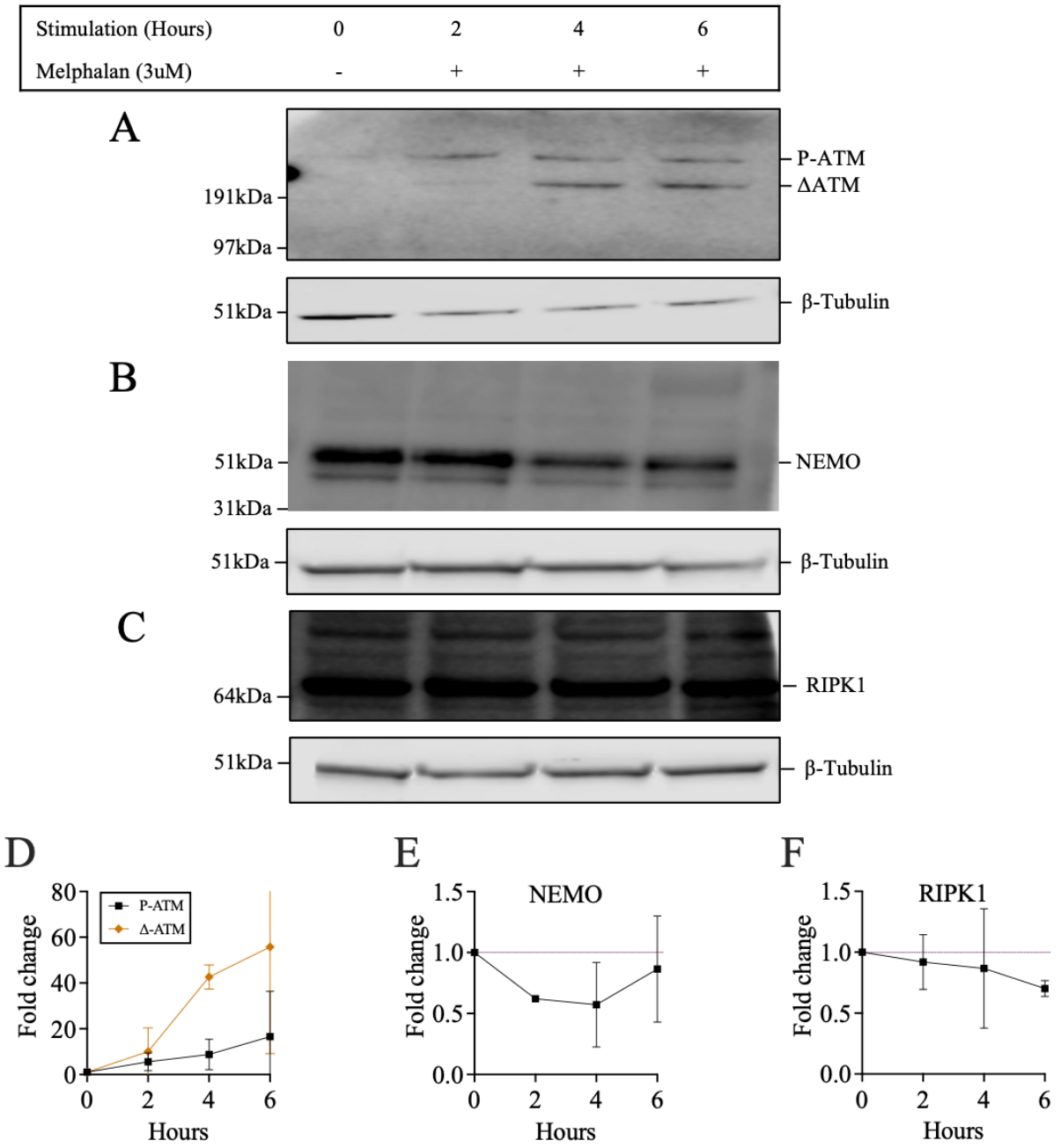

Figure 3.1: ATM, NEMO, and RIPK1 in melphalan-induced stress. Immunoblotting for P-ATM (Ser1981), NEMO, and RIPK1 levels in INA-6 cells treated with 10uM melphalan in a time series. The cells received treatment for either 2, 4, or 6 hours, and were then lysed and subjected to SDS-PAGE and western blotting. The negative control is treated with Ethanol and β-tubulin serves as loading control for relative protein quantities. **A/B/C.** One representative membrane out of three independent replications for P-ATM, NEMO, and RIPK1 respectively. Showing bands on membranes developed in an Odyssey LI-COR CLx system. **D/E/F.** Graphical illustration of the quantitative analysis done for P-ATM and ΔATM/NEMO/RIPK2 expression levels on Image Studio™ Software. Fold change calculated from three independent replications with values normalized to loading control. Whiskers represent the standard deviation between replications. The purple stippled line represents the untreated control which is set to 1.

3.1.1 ATM is phosphorylated in INA-6 cells treated with melphalan

ATM is a critical part of the DNA damage response. Once the DNA damage is recognized, kinases undergo autophosphorylation at serine residue 1981 enabling downstream signaling (48, 49). Hence, this particular modification can be used as a DNA damage response marker.

Bands for P-ATM can be observed on the membrane from the earliest time point, 2-hours stimulation. The bands increase in strength with stimulation time. Another lower band approximately 240kDA was also present. This band, termed ΔATM, has previously been detected and be an indication for apoptosis. This could be observed after 2-hour stimulation and also increase with stimulation time (Figure 3.1 **A**). Quantification of the bands show an increase in both ATM Phosphorylation and cleavage with stimulation time compared to control (Figure 3.1 **D**)

3.1.2 NEMO is modified in INA-6 cells treated with melphalan

NEMO has been shown to have an essential role as the polyubiquitin-binding scaffold in the canonical NF-κB-pathway. Additionally, NEMO is also important in nuclear-derived NF-κB activation in concert with ATM. This nuclear-to-cytoplasmic signaling involves several nuclear PTMs of NEMO. The aforementioned modifications include ATM-independent SUMOylation (Lys277/309), ATM-dependent phosphorylation (Ser85), and Mono-ubiquitination (Lys277/309) (50).

The membrane shows NEMO-bands that decrease with stimulation until 4 hours, then the values normalize compared to the untreated control (Figure 3.1 **E**). At 6 hours a high-molecular band could be detected at approximately 55kDa, although no PTM's was observed apart from this (Figure 3.1 **B**).

3.1.3 RIPK1 remains unchanged in INA-6 cells treated with melphalan

In addition to being a molecular switch for apoptosis, RIPK1 has also been reported to be involved in some DNA-damage signaling. The ATM/NEMO/RIPK1 association can in some cases serve to regulate the cells fate. When RIPK1 is implicated in the genotoxic-stress response it is modified with K63-polyubiquitylation and serves as a protein hub for furthering the signal (51).

The RIPK1 bands on the representative membrane show a slight decrease with stimulation time compared to control (Figure 3.1 **E**). With increased signal, a smear can be observed above RIP, but there is no noticeable change in intensity from untreated to melphalan-treated (Figure 3.1 **C**).

3.2 Mapping the pathway downstream ATM phosphorylation

Data from our group show that melphalan activates several proteins downstream of TAK1. These include p38, JNK, p38, and p65 (Håland, *Unpublished*). It could be determined if these proteins are activated as a result of ATM kinase activity by using a chemical ATM kinase inhibitor.

3.2.1 Titration of ATM-inhibitor KU-55933 in INA-6 cells

Ku-55933 is a specific ATM kinase-inhibitor, more specifically an ATP-competitive inhibitor (52). It has a selectivity for ATM which is at least 100-fold greater than other kinases, which makes it especially suited for single agent-effect studies (53). Before proceeding with the experiment, the dose required for blocking the phosphorylation of ATM in myeloma cells needed to be defined. More specifically, the dose of inhibitor required for maintaining the standard amount of phosphorylated ATM in INA-6 cells treated with 10uM melphalan. The dose range used for the titration was found in literature from previous experiments with the inhibitor (52-54).

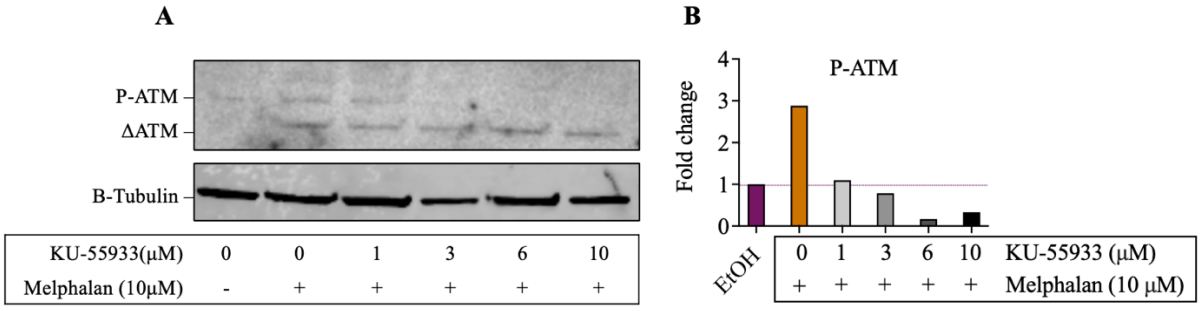

Figure 3.2.1: KU-55933 inhibits phosphorylation of ATM in doses higher than 3uM compared to control. Immunoblotting for P-ATM levels in INA-6 cells treated with melphalan (10 μM) for four hours as well as KU-55933 (1, 3, 6, and 10 μM) half an hour in advance. Cells were lysed and western blotted. The negative control is treated with ethanol while positive control is treated with melphalan. β-tubulin serves as a loading control for relative protein quantities. **A.** One representative membrane showing bands of P-ATM developed in an Odyssey LI-COR CLx system. **B.** Graphical illustration of the quantitative analysis done for P-ATM expression levels on Image Studio™ Software. Fold change calculated with values normalized to Ethanol loading control. Purple stippled line represents the untreated control which is set to 1. This experiment was only performed once.

The results from the titration with INA-6 cells are displayed in Figure 3.2.1. ATM is autophosphorylated, and the P-ATM bands on the representative membrane disappear with 3uM KU-55933 and higher doses, indicating that kinase activity is blocked (Figure 3.1.**A**). The fold change calculated from the quantification of bands is illustrated in (Figure 3.1.1 **B**). This substantiates that 3uM is sufficient to block ATM kinase activity in further experiments. Interestingly, the cleaved form of P-ATM was not affected by kinase-inhibition, indicating that this form is independent of ATM-kinase function.

3.2.2 ATM kinase activity affect both NF-κB and MAPK signaling

To test whether ATM is responsible for the signal transduction caused by melphalan in myeloma cells the following was done. INA-6 cells were seeded and treated with the ATM-inhibitor KU-55933 (3μM) and melphalan (10μM) for 4 hours. KU-55933 was added 30 minutes prior to melphalan. The cells were lysed assess activation of TAK1, p38 and IκB by phosphorylation by western blot analysis. A more detailed account of the protocol specification is described in the method section. The result from this experiment is illustrated in Figure 3.3.2 with one representative membrane for each protein and figures illustrating the quantification of this band.

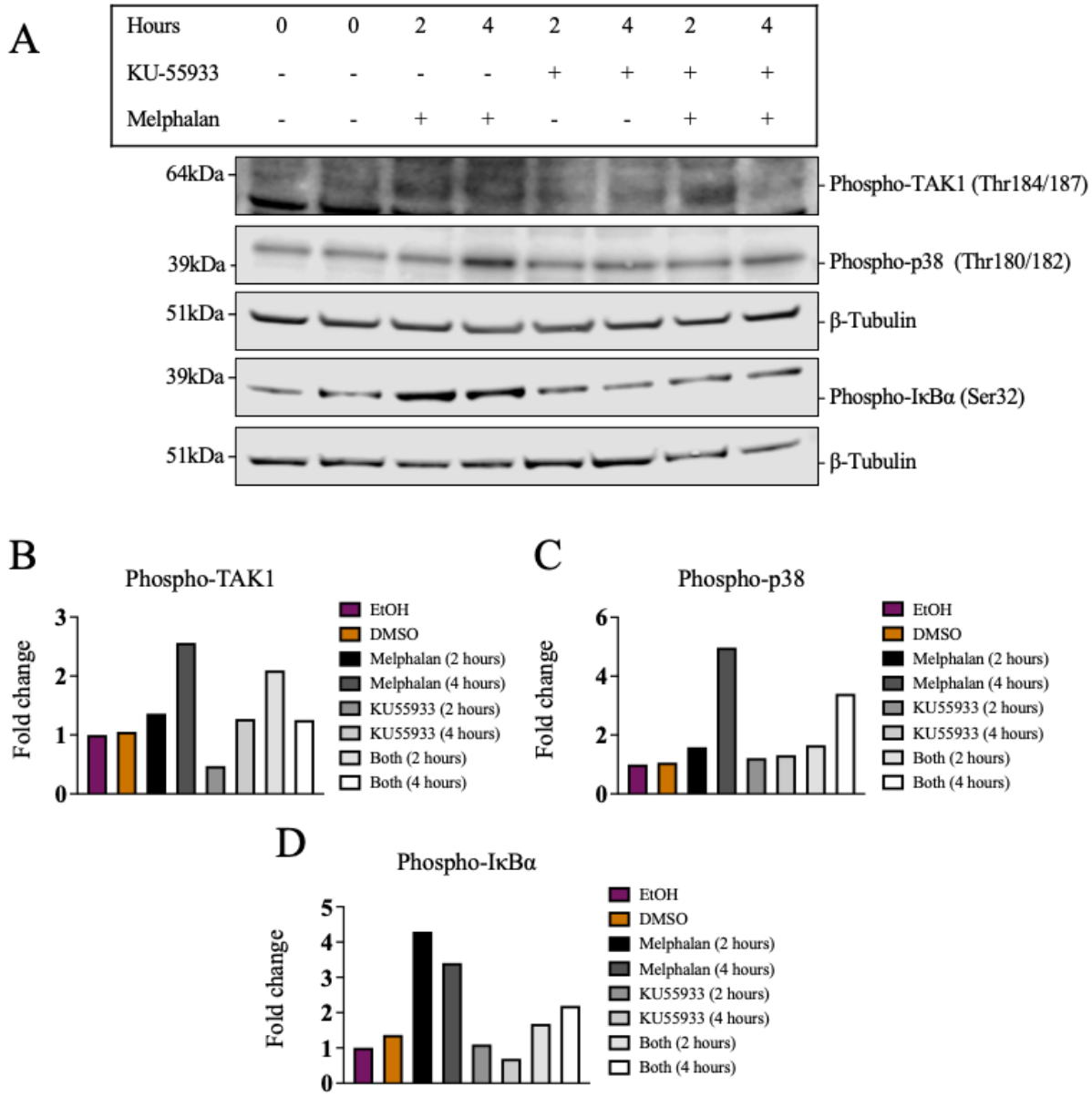

Figure 3.2.2: KU-55933 inhibits activation of intermediates downstream TAK1. Immunoblotting for Phospho-TAK1 (T184/187), Phospho-p38 (Thr180/Thr182), and Phospho-IκBα (Ser32) levels in INA-6 cells treated with either melphalan (10μM), KU55933 (3μM) or the combination of the two, for four hours. With KU-55933 half an hour in advance. Cells were lysed and western blotted. The negative control is treated with Ethanol and the second control with DMSO. β-tubulin serves as a loading control for relative protein quantities. **A.** One representative membrane showing bands of Phospho-TAK1 (T184/187), Phospho-p38 (Thr180/Thr182), and Phospho-IκBα (Ser32) developed in an Odyssey LI-COR CLx system. **B-D.** Graphical illustration of the quantitative analysis done for **B.** Phospho-TAK1 (T184/187) **C.** Phospho-p38(Thr180/Thr182) **D.** Phospho-IκBα (Ser32) expression levels on Image Studio™ Software. Fold change calculated with values normalized to Ethanol loading control. Due to time constraints, this experiment was only performed once.

3.2.3 Melphalan induced TAK1-phosphorylation is reduced by KU-55933

TAK1 is a positive regulator important for activation of NF-κB, as well as MAP kinases p38, JNK. This entails signaling survival through NF-κB and cellular stress-response through MAPK. However, its catalytic activity requires phosphorylation of tyrosine residue 184/187 (22).

Bands for Phospho-TAK1 can be observed at approximately 60kDa (Figure 3.2.2 **A**). The bands increase with melphalan stimulation compared to untreated control. The combination of the ATM-inhibitor and melphalan also increase phosphorylation compared to control but decreased compared to melphalan alone (Figure 3.2.2 **B**).

3.2.4 Melphalan induced p38-phosphorylation is reduced by KU-55933

p38 is responsible for phosphorylating factors in response to cellular stressors. The MAP kinase is indirectly a substrate of TAK1 (24). Activating p38 can have several tumor-promoting consequences like enhancing survival by developing resistance to stress and chemotherapeutic agents (55). Its activation requires dual phosphorylation of threonine- and tyrosine residues, 180 and 182 respectively (24).

Bands for Phospho-p38 can be observed at approximately 40kDa (Figure 3.2.3 **A**). The bands increase with melphalan stimulation compared to untreated control. Melphalan stimulation for 4-hours gives a 5-fold increase compared to control. The combination of the ATM-inhibitor and melphalan also increase phosphorylation compared to control, but decreased compared to melphalan alone (Figure 3.2.2 **C**).

3.2.5 Melphalan induced IκBα-phosphorylation is reduced by KU-55933

In canonical NF-κB-signaling the phosphorylation and degradation of IκBα are crucial for the release of p65 (13). When released, NF-κB dimer formation is made possible and regulation of genes occurs. The inhibitor is phosphorylated on serine residue 32 and marked for subsequent ubiquitination and degradation (14).

The results from one representative membrane and a figure constructed from quantification of the bands are illustrated in Figure 3.2.3 **A** and **D** respectively. Bands for Phospho-IκBα can be observed at approximately 35kDa. The bands increase in strength with melphalan stimulation compared to untreated control. Melphalan stimulation for 2-hours increased in strength more than 4-fold compared to 4-hours which is only 3-fold. KU-55933's decreases phosphorylation with 4 hours of stimulation. When stimulated with both agents phosphorylation increases, but lesser so than with melphalan alone (Figure 3.2.2 **D**).

3.3 Melphalan and NG25 influences SASP-secretion in INA-6 cells

Overactivation of NF-κB can cause the previously explained SASP-phenotype which is characterized by pro-inflammatory cytokines like MIP1α and MCP1. Cytokines can be hard to detect from MM cell lines, but preliminary data from the myeloma group and our group showed gene expression of MCP1 and MIP1α coding genes *CCL2* and *CCL3,* respectively (Håland, *Unpublished*). To test the effects of melphalan and TAK1-inhibition on the production of these pro-inflammatory cytokines in myeloma cells, the following was done. INA-6 cells were seeded and treated with melphalan, NG25, or the combination of the two. Then incubated for 12 hours before the cell-supernatant was collected. The protein concentration was then assessed by ELISA. A more detailed account of the protocol specification is described in the method section. The results from three independent experiments are illustrated in Figure 3.3 for **A.** MCP1 and **B.** MIP1α. All experiments are given in Supplementary Figure 4.

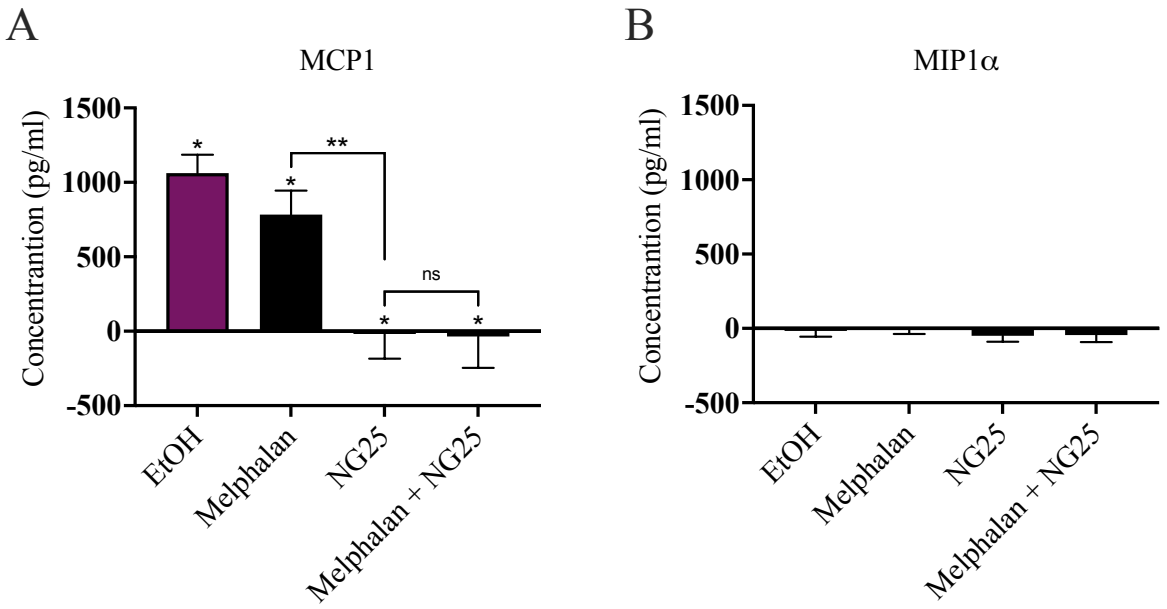

Figure 3.3: MCP1 and MIP1α production in INA-6 treated with melphalan, NG25, or the combination. INA-6 cells were treated with 10uM melphalan, 3uM NG25, or the combination of the two. Thereafter incubated for 12h before extracting cell-supernatant. The measurements of human MCP1 concentrations were done by MCP1 ELISA (DuoSet) assay. Results are given as technical triplicates from three independent experiments done with INA-6 cell lines. Asterisk denotes statistical significance as compared to the Ethanol treated control ($p<0.05$, One-way ANOVA). Double asterisks denote statistical significance between groups designated with brackets ($p<0,05$, Tukey multiple pairwise comparison test).

3.3.1 MCP1 production is reduced by both melphalan and NG25

There is a production above 1000 pg/ml of MCP1 in the ethanol-treated negative control. The melphalan-treated cells, however, exhibit a slight reduction (20%) in concentration compared to the control. A difference which was of statistical significance, but lesser than the other groups. The NG25 treated groups measurements were slim to none, with >100% reduction. Likewise, MCP1 concentration in the cells treated with the combination of NG25 and melphalan was equally low. Both these groups were of statistical significance compared to both the control and the melphalan-treated group. However, the difference between NG25s single-agent effect and the addition of melphalan was not significant (Figure 3.3 **A**). To summarize, INA-6 cells produce a significant amount of the pro-inflammatory mediator MCP1, which is reduced by both NG25 and Melphalan. The combination of the two agents has an adjacent effect to NG25 alone.

3.3.2 MIP1α production is not affected by Melphalan or NG25

There is an unmeasurable production of MIP1α in the ethanol-treated negative control. Compared to the control, the other groups showed no difference with statistical significance. Likewise, pairwise comparisons between the combinational treatment and the single-agent treatments showed no difference of statistical significance. MIP1α does not seem to be produced by the myeloma cell line INA-6 and this is also the case after treatment with melphalan and NG25 (Figure 3.3 **B**).

3.4 TAK1 inhibition and melphalan on Myc levels in myeloma

In multiple myeloma, Myc is activated and advances the malignant phenotype. Likewise, its activity increases with disease-stage. Some myeloma cells also develop a Myc-dependency, that if prevented can block proliferation and even activate apoptosis (56). An RNA-sequencing experiment executed by our group showed that NG25 reduced transcription of Myc-regulated genes (Håland, *Unpublished*). Myc activity is proportional to Myc protein levels. To test how TAK1 inhibition affects the Myc levels in myeloma cells, and whether there was an interaction between melphalan and NG25 that affects Myc activity, the following was done.

JJN3, ANBL-6, INA-6, and RPMI-8226 cells were seeded and treated with either melphalan (10μM), NG25 (2μM), or the combination of the two for four hours. The cells were lysed to assess protein quantity of Myc with western blot analysis. A more detailed account of the protocol specification is described in the method section. Three independent experiments are

performed. One representative experiment (Figure 3.4 **A**) and quantification of all three experiments (Figure 3.4 **B**) are shown. A complete set of membranes for all experiments are given in Supplementary Figure 5.

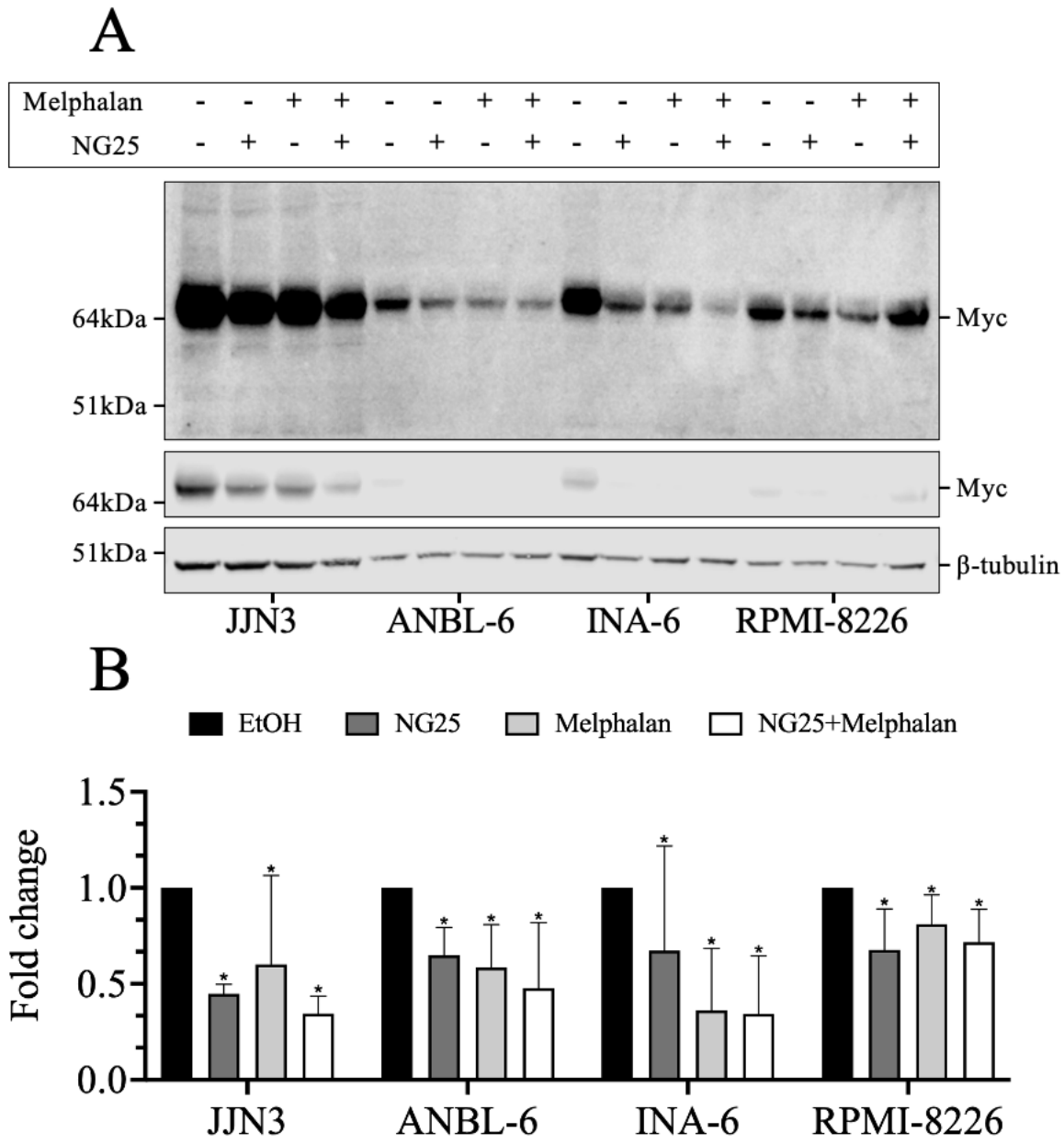

Figure 3.4: Melphalan and NG25 lowers Myc levels in myeloma cell lines
Immunoblotting for Myc levels in JJN3, ANBL-6, INA-6, and RPMI-8226 cells treated with either NG25 (2μM), Melphalan (10μM), or the combination of the two. Cells were treated for 4-hours, lysed and western blotted. The negative control is treated with ethanol and β-tubulin serves as loading control for relative protein quantities. **A.** One representative membrane out of three independent experiments is shown. Showing bands of Myc developed in an Odyssey LI-COR CLx system. **B.** Graphical illustration of the quantitative analysis done for Myc expression levels on Image Studio™ Software. Fold change calculated from three independent replications with values normalized to loading control. Fold change calculated from three independent replications with values normalized to loading control. Whiskers represents standard deviation between replications. Asterisk denotes statistical significance as compared to the ethanol-treated control ($p<0.05$, One-way ANOVA)

3.4.1 TAK1 inhibition and melphalan lowers Myc levels in myeloma cell lines

The results from three independent experiments are illustrated in Figure 3.4.1. The Myc bands on the representative membrane show a decrease with stimulation of both stimuli compared to control. Myc levels are lowered in all four cell lines with both agents, separately and combined (Figure 3.4.1 **A**). The two drugs have an inverse-synergistic effect on the Myc levels. INA-6 and JJN-3 are the most affected, reaching fold change values of >0,6 (Figure 3.4.1 **E**).

4 Discussion

The aim of this thesis was divided into three different research questions, aimed at strengthening knowledge of melphalan-induced signaling in MM. Being that melphalan is still commonly used in myeloma therapy and development of minimal residual disease is a pressing issue. The cells that manage to escape the apoptotic state that melphalan induces do so by signaling survival and triggering innate stress-response mechanisms. At the center of this is NF-κB and MAPKs, both of which are regulated by TAK1. Previous studies have shown that TAK1-inhibition not only neutralizes the production of proinflammatory cytokines but sensitizes myeloma cells for therapy (45). On top of this, our own studies have shown that high expression of *MAP3K7* is correlated with worsened prognosis, and that TAK1-inhibitors such as NG25 and 5z7 are cytotoxic to myeloma cell-lines and patient samples, alone and in combination with melphalan (Håland, *Unpublished*). The data suggest that myeloma cells utilize NF-κB to evade apoptosis triggered by genome instability.

4.1 Auto-phosphorylation of ATM initiates the TAK1/NF-κB/MAPK-cascade in response to melphalan in myeloma

The first research question formulated was to identify the molecular mechanism that orchestrates the melphalan-induced TAK1 activation. This thesis focused on the stress caused by melphalan. This was done by observing the proteins usually involved in this kind of signaling. Namely ATM, NEMO, and RIPK1 were examined for PTM's and protein quantity. The experiments revealed that melphalan induced phosphorylation of ATM, a known transducer of the DNA damage response. Phosphorylation of serine residue 1981, a modification that is known to be auto induced. Phospho-ATM is simultaneously cleaved producing the product ΔATM, approximately 240kDA large. This specific cleavage of ATM has been found to be the product of caspase 3, a process triggered in cells induced to undergo apoptosis (57).

This supports the previous finding of our group which states that melphalan induces a combination of mitochondrial and caspase 8-dependent apoptosis. Seeing that caspase 3 is cleaved by caspase 8 in RIPK1-dependent apoptosis. Even if the cells were treated with sublethal doses of melphalan, it could be expected that a portion of the cells will undergo apoptosis. Titration of the ATM-inhibitor KU55933 offered additional information about ΔATM. The cleavage of ATM seemed to be independent of ATM-kinase activity. ΔATM quantity increased despite total inhibition of the kinase. This is in line with the findings of Smith

et al. (1999) which suggest that ΔATM is a kinase-inactive protein, but the DNA-binding properties remain. More interestingly is their suggestion that ΔATM function in a *trans*-dominant negative fashion, interfering with DNA-repair mechanisms. However, the results of this thesis show that ATM is activated by melphalan in myeloma cell lines and is important for the downstream activation of NF-κB and MAPK.

The results were less clear for the aforementioned NEMO and RIPK1. Melphalan induced a measurable reduction in the protein levels for both NEMO and RIPK1. Although the experiment intended to observe if the proteins are modified as a result of melphalan treatment. Since the literature points to several PTM's important for signal transduction. In some of the replications, a band does appear approximately 10kDa above NEMO after 6 hours of stimulation. This is of interest since NEMO has been said to be both SUMOylated and monoubiquitinated in the DNA damage response. These modifications usually add additional 8,5 and 15kDA to the protein when immunoblotted respectively (58, 59). This is speculation non the less, more conclusive experiments remain to be done.

The difference in protein levels, although consistent, is not significant enough to determine. However, this may stem from the formation of complexes, which is a pillar of their way of signaling. Since some protein complexes are not dissolved in the lysis buffer and will as a consequence be removed with DNA and membranes during centrifugation. A solution could be to lyse this pellet and dissolve it in 8M urea to break up hydrogen bonds. Alternatively, co-immunoprecipitation could be applied to test for complex formation.

4.2 Melphalan activates TAK1, p38, and NF-κB through ATM

Data from our group show that melphalan activates several proteins downstream of TAK1. These include p38 and p65, proteins responsible for signaling MAPK and NF-κB (Håland, *Unpublished*). As we observed that melphalan activated ATM, we then wanted to investigate whether ATM activity was necessary for MAPK and NF-κB activation. This was done by selecting the same collection of proteins and their known modifications. By blocking the kinase activity of ATM, it could be determined if these proteins are activated as a result of ATM kinase activity.

This experiment did not yield three independent replications due to time constraints. Therefore, these results are not of a quality to draw conclusions from. However, as preliminary data, they are interesting and show a clear trend. Activation of TAK1 and one protein involved in each of the downstream pathways were measured. The MAPK p38 is phosphorylated and thereby activated in response to melphalan, increasingly with stimulation time. This was clearly reduced by the ATM inhibitor.

Phosphorylation of IκBα representing NF-κB activation is used because of the high turnover of p65. NF-κB activation is difficult to spot with immunoblotting since it is fast-acting. With the presence of IκBα, the DNA-bound NF-κB complex has a half-life of 3 min (60). It is therefore appropriate to rely on more predictable factors that reflect its activation. IκBα was also phosphorylated in response to melphalan alone and in combination with KU-55933. The combinational therapy caused lower levels of phosphorylation than melphalan alone.

TAK1 exhibit the same pattern where the combinational therapy leads to less phosphorylation than melphalan alone. This indicates that ATM is responsible for the activation of TAK1 and its downstream pathways in the melphalan-stress response. The proteins are however activated only to a lesser degree, giving a partial effect. One explanation might be crosstalk between pathways, which can compensate for the loss of function.

4.3 Both NG25 and melphalan reduces secretion of proinflammatory cytokine MCP1 in myeloma cells

Overactivation of NF-κB can cause the previously explained SASP-phenotype, which is characterized by pro-inflammatory cytokines like MIP1α and MCP1. Cytokines can be hard to detect from MM cell lines, but preliminary data from the myeloma group and our group showed gene expression of MCP1 and MIP1α coding genes *CCL2* and *CCL3,* respectively (Håland, *Unpublished*). In MM it can be favorable for the tumor cells to create an inflammatory microenvironment, granting the tumor cells with the signals needed for survival. It is also known that both MAPK and NF-κB are linked to the production of cytokines. To test the effects of melphalan and TAK1-inhibition on the production of these proinflammatory cytokines in myeloma cells, ELISA was applied.

Only one of the cytokines yielded noteworthy results, MIP1α levels were too low to measure any significant change. The MCP1 production in the myeloma cell line was surprisingly enough, already turned on. Myeloma cells have, as mentioned repeatedly during this thesis, often constitutively active NF-κB. Additionally, this cell line gets the proinflammatory cytokine IL-6 supplied in its medium due to dependency. A molecule known to stimulate NF-κB signaling. This might also affect the concentration in the medium measured in the untreated control.

Contrary to initial assumptions, stimulating with melphalan decreased this production MCP1, but how this occur is less clear. We used a melphalan-dose that previously yielded a 20% decrease in cell viability in experiments done by our group (Håland, *Unpublished*). This could explain some or all of the reduction in MCP1 concentration. Stimulation with TAK1-inhibitor NG25 brought some clarification to the results, since inhibition irradicated the production of MCP1 completely. This substantiates that NF-κB and/or MAPK are responsible for the *CCL2*-upregulation observed. Hence, another explanation for melphalan reducing it might be that the strength of the signal induced is lesser than the one already in place. Where the TAK1 inhibition is concerned, this is in line with the literature, where NF-κB is found to be important for *CCL2* production. The same paper also states that MAPKs JNK and p38 may also be involved, but not ERK (61). In our own previous work, we see that melphalan induces activation of the first two (Håland, *Unpublished*).

To better identify SASP in myeloma cells treated with melphalan, a more comprehensive analysis is necessary. Commonly used strategies include establishing the presence of primary and secondary markers since no one characteristic solely defines SASP. Primary markers include cell cycle arrest and morphological changes. For instance, MTT-assays can be utilized to identify cell cycle arrest after treatment. Senescence-associated β-galactosidase (SA-β-Gal) staining is a reliable example of identifying morphological changes. These results of this thesis speak to secondary markers, such as cytokine production and DNA-damage response. Other secondary characteristics include apoptosis evasion. Due to TAK1s role in upregulating the SASP phenotype, it would be interesting to see how it affects these SASP hallmarks.

4.4 Both NG25 and melphalan reduces Myc levels in multiple myeloma cell lines

In multiple myeloma, Myc activity increases with the disease stage. Some myeloma cells also develop a Myc-dependency, that if prevented can block proliferation and even activate apoptosis (56). An RNA-sequencing experiment executed by our group showed that NG25 reduced transcription of Myc-regulated genes in INA-6 cells (Håland, *Unpublished*). Due to the importance of Myc in multiple myeloma, we wanted to find out if this was reflected in the level of Myc activity, and whether it applied to other MM cell lines. To test this, both melphalan and TAK1-inhibitor NG25 were given to four different cell lines, and Myc protein level was measured as it correlates with activity. Interestingly the two agents affected Myc levels the same way, significantly reducing it in all cell lines. Contradictory to the evidence since one stimulant is supposed to turn off the pathway that the other activates. This leads to the conclusion that Myc levels are regulated in an alternative fashion outside the scope of NF-κB and MAPK. Melphalan did not however reduce the expression of Myc-related genes in the RNA-sequencing experiment (Håland, *Unpublished*).

NF-κB has been shown to be co-regulated with Myc in several studies (62-65). Including one that found NEMO to directly interact with Myc degradation, stabilizing it (66). The contribution of NEMO in the melphalan-induced signaling might interfere with the aforementioned mechanism. More research remains to be done concerning Myc- NF-κB co-regulation. The mechanisms behind the down-regulation of Myc would need to be established, as well as replicating this in myeloma patient samples.

5 Conclusion

In this study, we showed for the first time that the DNA-damage melphalan induces in myeloma cells activates a response orchestrated by the nuclear kinase ATM. ATM is activated by autophosphorylation of serine residue 1981. Experiments indicate that NEMO also is involved, but more data is necessary to establish this. To further clarify, it would be interesting to see if ELKS are poly-ubiquitinated as an alternative to RIPK1 in this pathway. Modification of NEMO could also be clarified by the use of immunoprecipitation or antibodies for the different modifications the literature points to. The same activation is responsible for the downstream signaling activating NF-κB and MAPK. Though more rigid data is needed to conclude. Our studies also demonstrate that the melphalan stress response down-regulates the production of pro-inflammatory cytokine MCP1. TAK1-inhibition has the same effect only more potent. Lastly, this stress response down-regulates the protein levels of the oncogenic transcription factor Myc. These results are promising since it supports that TAK1-inhibition can downregulate both NF-κB, MAPK and Myc signaling; all important in the pathogenesis of MM. Melphalan and TAK1 inhibition remain an interesting potential combinational therapy.

6 Supplementary

Figure 1.

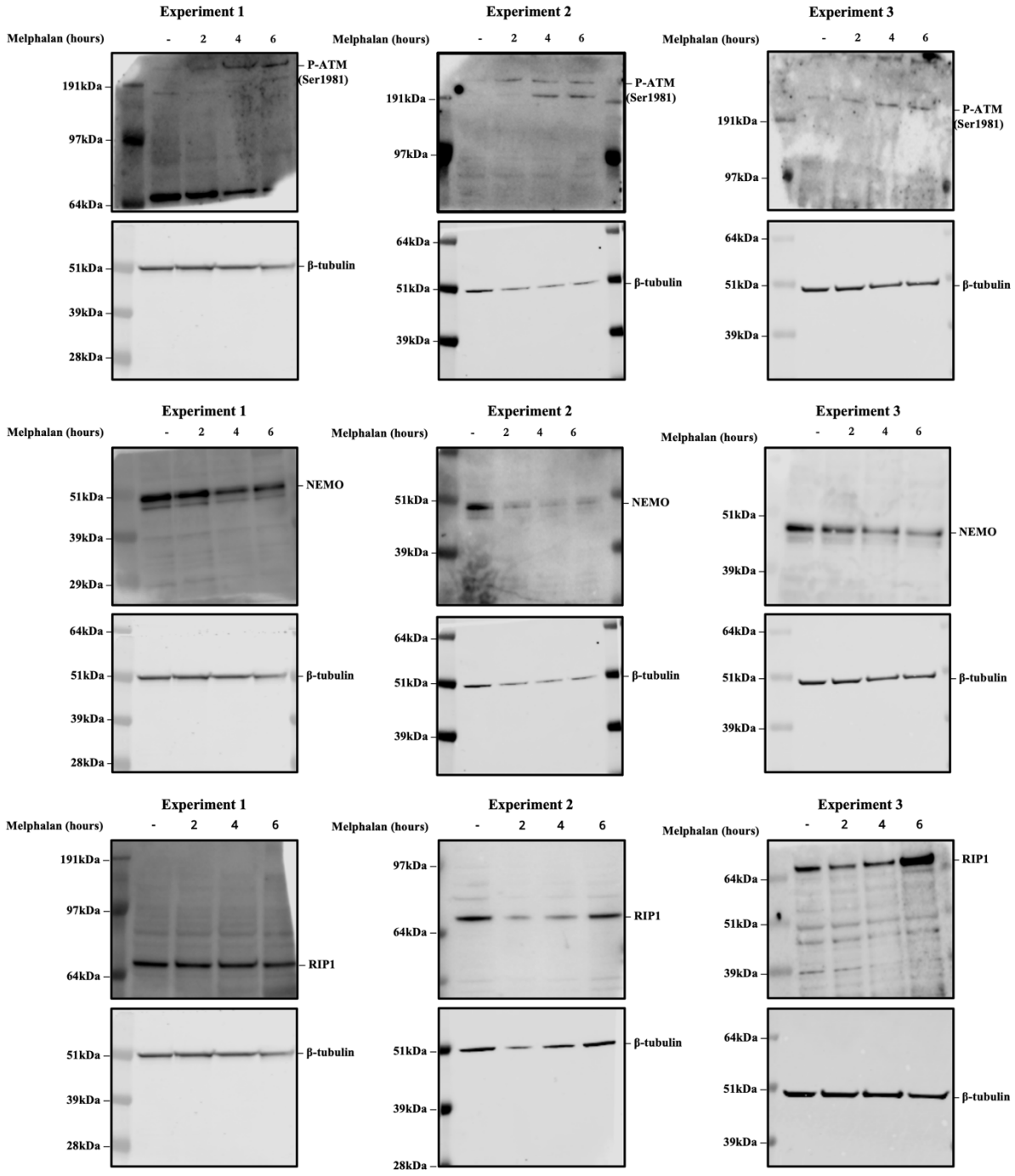

Figure 2.

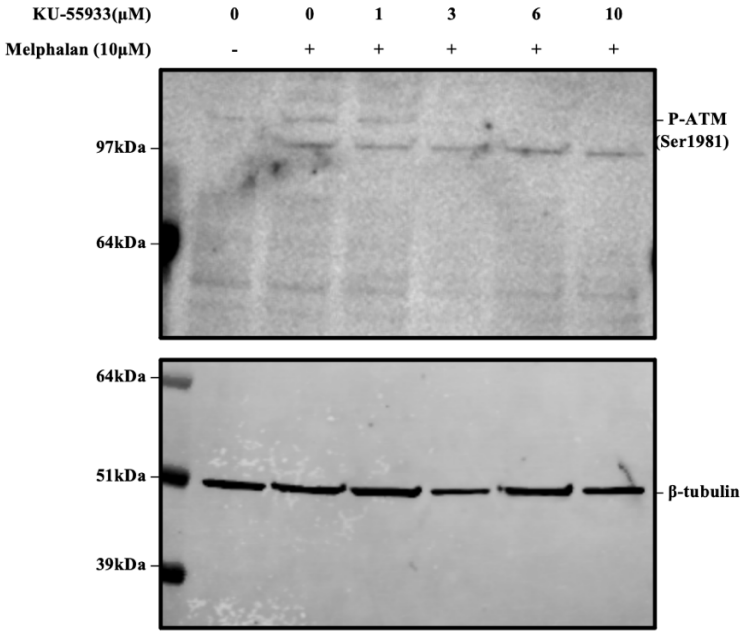

Figure 3.

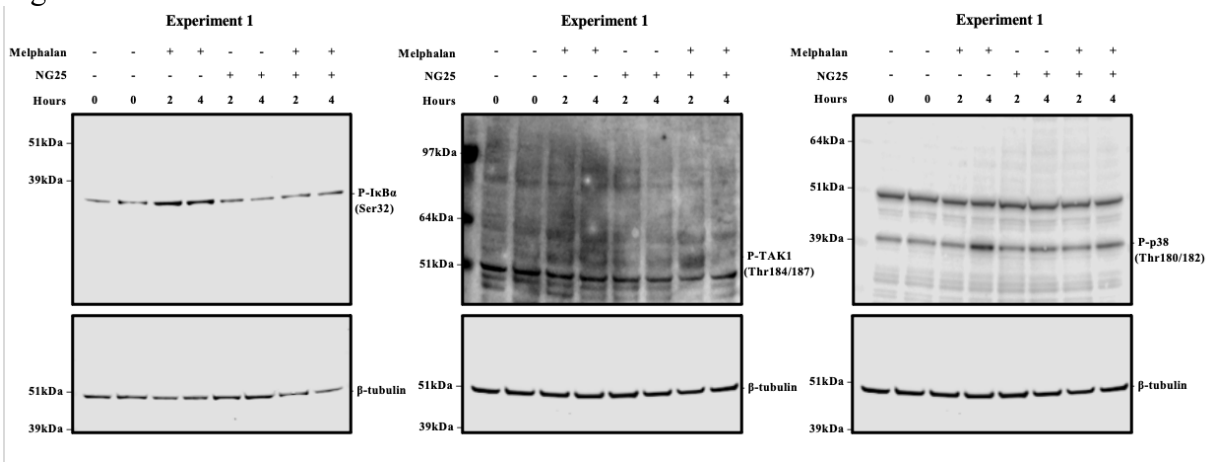

Figure 4

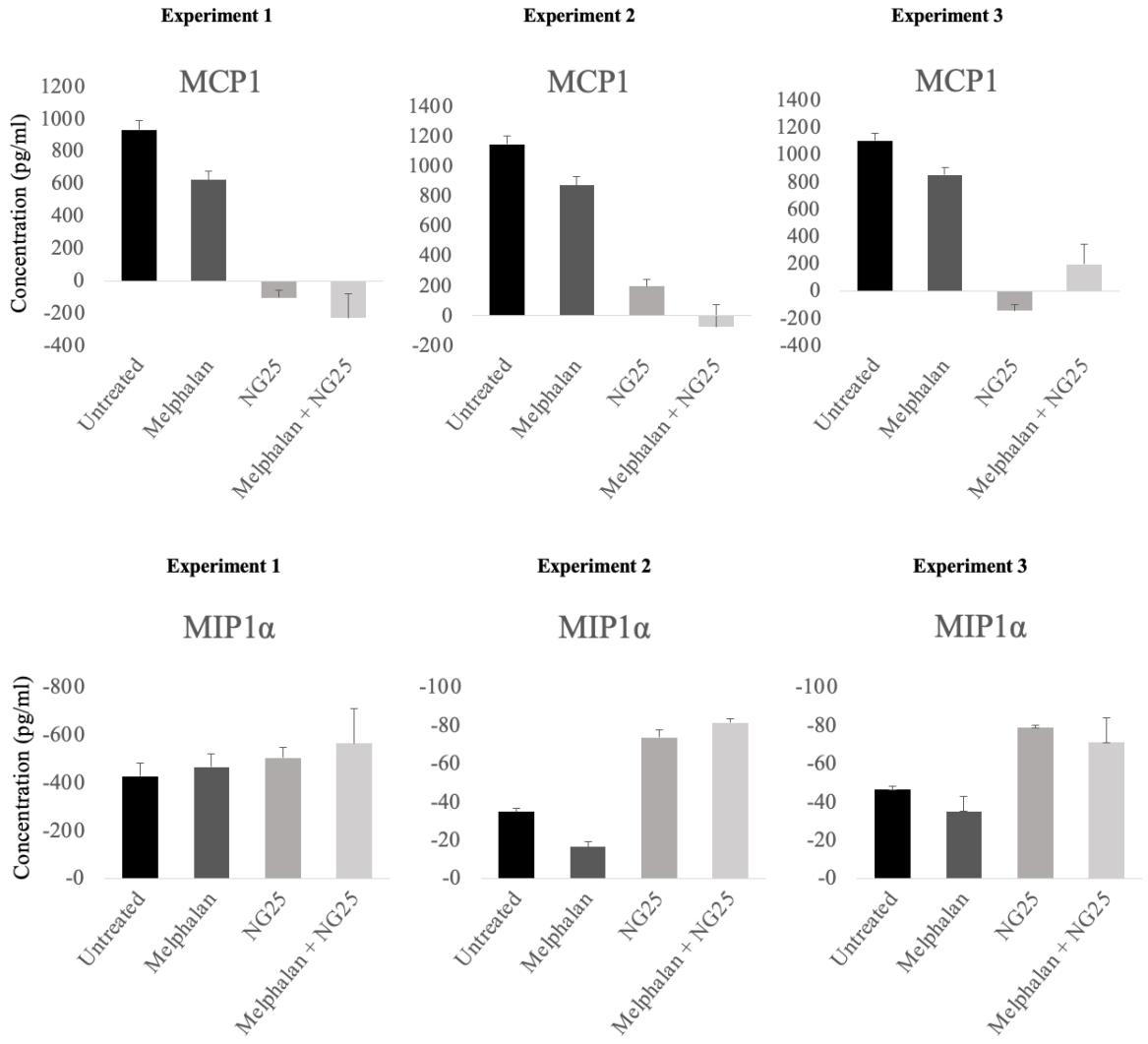

Figure 5

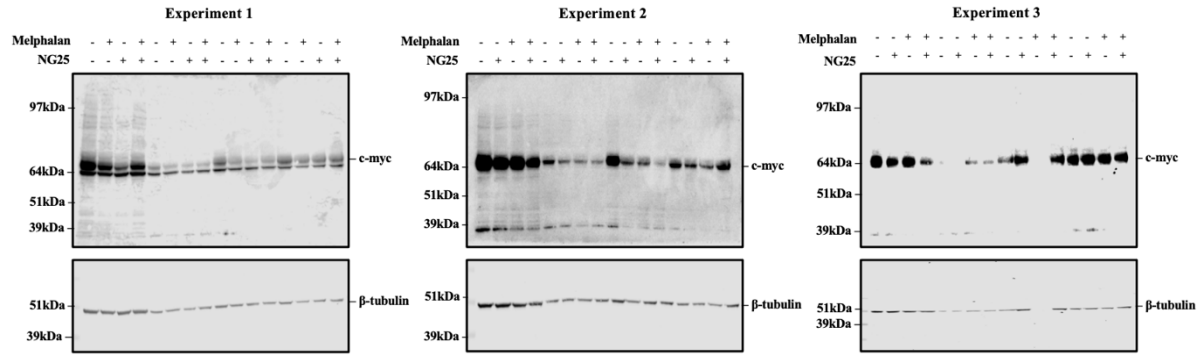

7 References

1. Palumbo A, Anderson K. Multiple Myeloma. New England Journal of Medicine. 2011;364(11):1046–60.
2. Kazandjian D. Multiple myeloma epidemiology and survival: A unique malignancy. Seminars in Oncology. 2016;43(6):676–81.
3. Al–Farsi K. Multiple myeloma: an update. Oman Med J. 2013;28(1):3–11.
4. Kostopoulos IV, Ntanasis–Stathopoulos I, Gavriatopoulou M, Tsitsilonis OE, Terpos E. Minimal Residual Disease in Multiple Myeloma: Current Landscape and Future Applications With Immunotherapeutic Approaches. Front Oncol. 2020;10:860.
5. Dehghanifard A, Kaviani S, Abroun S, Mehdizadeh M, Saiedi S, Maali A, et al. Various Signaling Pathways in Multiple Myeloma Cells and Effects of Treatment on These Pathways. Clin Lymphoma Myeloma Leuk. 2018;18(5):311–20.
6. Demchenko YN, Kuehl WM. A critical role for the NFkB pathway in multiple myeloma. Oncotarget. 2010;1(1):59–68.
7. Dolcet X, Llobet D, Pallares J, Matias–Guiu X. NF–kB in development and progression of human cancer. Virchows Arch. 2005;446(5):475–82.
8. Xia Y, Shen S, Verma IM. NF–κB, an active player in human cancers. Cancer Immunol Res. 2014;2(9):823–30.
9. Hanahan D, Weinberg RA. Hallmarks of cancer: the next generation. Cell. 2011;144(5):646–74.
10. Li ZW, Chen H, Campbell RA, Bonavida B, Berenson JR. NF–kappaB in the pathogenesis and treatment of multiple myeloma. Curr Opin Hematol. 2008;15(4):391–9.
11. Mercurio F, Manning AM. NF–κB as a primary regulator of the stress response. Oncogene. 1999;18(45):6163–71.
12. Hayden MS, Ghosh S. Shared principles in NF–kappaB signaling. Cell. 2008;132(3):344–62.
13. Mitchell S, Vargas J, Hoffmann A. Signaling via the NFκB system. Wiley Interdiscip Rev Syst Biol Med. 2016;8(3):227–41.
14. Yu H, Lin L, Zhang Z, Zhang H, Hu H. Targeting NF–κB pathway for the therapy of diseases: mechanism and clinical study. Signal Transduct Target Ther. 2020;5(1):209.
15. Brenner D, Blaser H, Mak TW. Regulation of tumour necrosis factor signalling: live or let die. Nat Rev Immunol. 2015;15(6):362–74.
16. Ofengeim D, Yuan J. Regulation of RIP1 kinase signalling at the crossroads of inflammation and cell death. Nat Rev Mol Cell Biol. 2013;14(11):727–36.
17. Mihaly SR, Ninomiya–Tsuji J, Morioka S. TAK1 control of cell death. Cell Death Differ. 2014;21(11):1667–76.

18. Humphries F, Yang S, Wang B, Moynagh PN. RIP kinases: key decision makers in cell death and innate immunity. Cell Death Differ. 2015;22(2):225–36.
19. Wong RS. Apoptosis in cancer: from pathogenesis to treatment. J Exp Clin Cancer Res. 2011;30(1):87.
20. Podder B, Guttà C, Rožanc J, Gerlach E, Feoktistova M, Panayotova–Dimitrova D, et al. TAK1 suppresses RIPK1–dependent cell death and is associated with disease progression in melanoma. Cell Death Differ. 2019;26(12):2520–34.
21. Aashaq S, Batool A, Andrabi KI. TAK1 mediates convergence of cellular signals for death and survival. Apoptosis. 2019;24(1–2):3–20.
22. Mukhopadhyay H, Lee NY. Multifaceted roles of TAK1 signaling in cancer. Oncogene. 2020;39(7):1402–13.
23. Dai L, Aye Thu C, Liu XY, Xi J, Cheung PC. TAK1, more than just innate immunity. IUBMB Life. 2012;64(10):825–34.
24. Roux PP, Blenis J. ERK and p38 MAPK–activated protein kinases: a family of protein kinases with diverse biological functions. Microbiol Mol Biol Rev. 2004;68(2):320–44.
25. Johnson GL, Lapadat R. Mitogen–activated protein kinase pathways mediated by ERK, JNK, and p38 protein kinases. Science. 2002;298(5600):1911–2.
26. Kishimoto K, Matsumoto K, Ninomiya–Tsuji J. TAK1 mitogen–activated protein kinase kinase kinase is activated by autophosphorylation within its activation loop. J Biol Chem. 2000;275(10):7359–64.
27. Burotto M, Chiou VL, Lee JM, Kohn EC. The MAPK pathway across different malignancies: a new perspective. Cancer. 2014;120(22):3446–56.
28. Yang J, He J, Wang J, Cao Y, Ling J, Qian J, et al. Constitutive activation of p38 MAPK in tumor cells contributes to osteolytic bone lesions in multiple myeloma. Leukemia. 2012;26(9):2114–23.
29. Bretones G, Delgado MD, León J. Myc and cell cycle control. Biochim Biophys Acta. 2015;1849(5):506–16.
30. Pelengaris S, Khan M, Evan G. c–MYC: more than just a matter of life and death. Nat Rev Cancer. 2002;2(10):764–76.
31. Dang CV. MYC on the path to cancer. Cell. 2012;149(1):22–35.
32. Barbosa R, Xu A, D'Andrea D, Copley F, Patel H, Chakravarty P, et al. Co–activation of NF–κB and MYC renders cancer cells addicted to IL6 for survival and phenotypic stability. bioRxiv. 2020:2020.04.12.038414.
33. Falco P, Bringhen S, Avonto I, Gay F, Morabito F, Boccadoro M, et al. Melphalan and its role in the management of patients with multiple myeloma. Expert Review of Anticancer Therapy. 2007;7(7):945–57.
34. Röllig C, Knop S, Bornhäuser M. Multiple myeloma. Lancet. 2015;385(9983):2197–208.

35. Makin G, Hickman JA. Apoptosis and cancer chemotherapy. Cell Tissue Res. 2000;301(1):143–52.
36. Yang Y, Xia F, Hermance N, Mabb A, Simonson S, Morrissey S, et al. A cytosolic ATM/NEMO/RIP1 complex recruits TAK1 to mediate the NF–kappaB and p38 mitogen–activated protein kinase (MAPK)/MAPK–activated protein 2 responses to DNA damage. Mol Cell Biol. 2011;31(14):2774–86.
37. Wu ZH, Wong ET, Shi Y, Niu J, Chen Z, Miyamoto S, et al. ATM– and NEMO–dependent ELKS ubiquitination coordinates TAK1–mediated IKK activation in response to genotoxic stress. Mol Cell. 2010;40(1):75–86.
38. Hinz M, Stilmann M, Arslan S, Khanna KK, Dittmar G, Scheidereit C. A cytoplasmic ATM–TRAF6–cIAP1 module links nuclear DNA damage signaling to ubiquitin–mediated NF–κB activation. Mol Cell. 2010;40(1):63–74.
39. Salminen A, Kauppinen A, Kaarniranta K. Emerging role of NF–κB signaling in the induction of senescence–associated secretory phenotype (SASP). Cell Signal. 2012;24(4):835–45.
40. Lopes–Paciencia S, Saint–Germain E, Rowell MC, Ruiz AF, Kalegari P, Ferbeyre G. The senescence–associated secretory phenotype and its regulation. Cytokine. 2019;117:15–22.
41. Zhang B, Fu D, Xu Q, Cong X, Wu C, Zhong X, et al. The senescence–associated secretory phenotype is potentiated by feedforward regulatory mechanisms involving Zscan4 and TAK1. Nat Commun. 2018;9(1):1723.
42. Saleh T, Bloukh S, Carpenter VJ, Alwohoush E, Bakeer J, Darwish S, et al. Therapy–Induced Senescence: An "Old" Friend Becomes the Enemy. Cancers (Basel). 2020;12(4).
43. Taniguchi K, Karin M. NF–κB, inflammation, immunity and cancer: coming of age. Nat Rev Immunol. 2018;18(5):309–24.
44. Faget DV, Ren Q, Stewart SA. Unmasking senescence: context–dependent effects of SASP in cancer. Nat Rev Cancer. 2019;19(8):439–53.
45. Pinto V, Bergantim R, Caires HR, Seca H, Guimarães JE, Vasconcelos MH. Multiple Myeloma: Available Therapies and Causes of Drug Resistance. Cancers (Basel). 2020;12(2).
46. Chesi M, Mirza NN, Garbitt VM, Sharik ME, Dueck AC, Asmann YW, et al. IAP antagonists induce anti–tumor immunity in multiple myeloma. Nat Med. 2016;22(12):1411–20.
47. Chabner BA, Roberts TG, Jr. Timeline: Chemotherapy and the war on cancer. Nat Rev Cancer. 2005;5(1):65–72.
48. Lee JH, Paull TT. Activation and regulation of ATM kinase activity in response to DNA double–strand breaks. Oncogene. 2007;26(56):7741–8.

49. Tang X, Hui ZG, Cui XL, Garg R, Kastan MB, Xu B. A novel ATM–dependent pathway regulates protein phosphatase 1 in response to DNA damage. Mol Cell Biol. 2008;28(8):2559–66.
50. Miyamoto S. Nuclear initiated NF–κB signaling: NEMO and ATM take center stage. Cell Res. 2011;21(1):116–30.
51. McCool KW, Miyamoto S. DNA damage–dependent NF–κB activation: NEMO turns nuclear signaling inside out. Immunol Rev. 2012;246(1):311–26.
52. Hickson I, Zhao Y, Richardson CJ, Green SJ, Martin NM, Orr AI, et al. Identification and characterization of a novel and specific inhibitor of the ataxia–telangiectasia mutated kinase ATM. Cancer Res. 2004;64(24):9152–9.
53. Herrero AB, Gutiérrez NC. Targeting Ongoing DNA Damage in Multiple Myeloma: Effects of DNA Damage Response Inhibitors on Plasma Cell Survival. Front Oncol. 2017;7:98.
54. Khalil HS, Tummala H, Hupp TR, Zhelev N. Pharmacological inhibition of ATM by KU55933 stimulates ATM transcription. Exp Biol Med (Maywood). 2012;237(6):622–34.
55. Martínez–Limón A, Joaquin M, Caballero M, Posas F, de Nadal E. The p38 Pathway: From Biology to Cancer Therapy. Int J Mol Sci. 2020;21(6).
56. Holien T, Våtsveen TK, Hella H, Waage A, Sundan A. Addiction to c–MYC in multiple myeloma. Blood. 2012;120(12):2450–3.
57. Smith GC, dAdda di Fagagna F, Lakin ND, Jackson SP. Cleavage and inactivation of ATM during apoptosis. Mol Cell Biol. 1999;19(9):6076–84.
58. Hilgarth RS, Sarge KD. Detection of sumoylated proteins. Methods Mol Biol. 2005;301:329–38.
59. Xu G, Jaffrey SR. Proteomic identification of protein ubiquitination events. Biotechnol Genet Eng Rev. 2013;29(1):73–109.
60. Saccani S, Marazzi I, Beg AA, Natoli G. Degradation of promoter–bound p65/RelA is essential for the prompt termination of the nuclear factor kappaB response. J Exp Med. 2004;200(1):107–13.
61. Thompson WL, Van Eldik LJ. Inflammatory cytokines stimulate the chemokines CCL2/MCP–1 and CCL7/MCP–3 through NFkB and MAPK dependent pathways in rat astrocytes [corrected]. Brain Res. 2009;1287:47–57.
62. Tanaka H, Matsumura I, Ezoe S, Satoh Y, Sakamaki T, Albanese C, et al. E2F1 and c–Myc potentiate apoptosis through inhibition of NF–kappaB activity that facilitates MnSOD–mediated ROS elimination. Mol Cell. 2002;9(5):1017–29.
63. You Z, Madrid LV, Saims D, Sedivy J, Wang CY. c–Myc sensitizes cells to tumor necrosis factor–mediated apoptosis by inhibiting nuclear factor kappa B transactivation. J Biol Chem. 2002;277(39):36671–7.

64. Grumont RJ, Strasser A, Gerondakis S. B cell growth is controlled by phosphatidylinosotol 3–kinase–dependent induction of Rel/NF–kappaB regulated c–myc transcription. Mol Cell. 2002;10(6):1283–94.
65. Keller U, Nilsson JA, Maclean KH, Old JB, Cleveland JL. Nfkb 1 is dispensable for Myc–induced lymphomagenesis. Oncogene. 2005;24(41):6231–40.
66. Kim BY, Yang JS, Kwak SY, Zhang XK, Han YH. NEMO stabilizes c–Myc through direct interaction in the nucleus. FEBS Lett. 2010;584(22):4524–30.